Modified Bipyridines: 5,5′-Diamino-2,2′-bipyridine Metal Complexes Assembled into Multidimensional Networks via Hydrogen Bonding and π–π Stacking Interactions

Christoph Janiak,*[a] Stephan Deblon,[a] He-Ping Wu,[a] Mario J. Kolm,[a] Peter Klüfers,*[b] Holger Piotrowski,[b] and Peter Mayer[b]

A new synthetic route for the synthesis of 5,5′-diamino-2,2-bipyridine (5) based on the coupling of 2-chloro-5-aminopyridine in the presence of $NiCl_2 \times 6 H_2O/PPh_3/Zn$ in dimethylformamide is described. The reactions of the potentially ambidentate ligand 5 with salts of the transition metals Mn, Fe, Ni, Cu, Zn, Ag, and Cd gave a variety of 13 metal–ligand complexes depending on the anion, the crystallization conditions and the metal-to-ligand ratio. The complexes obtained were characterized by thermal analyses, NMR including [113]Cd-NMR, IR, and for the iron complex [57]Fe-Mößbauer spectroscopy. The structure of eight of the compounds was elucidated by X-ray crystallography. All of these metal complexes show a bipyridine–metal coordination. The amino functionality was never involved in metal coordination. The intermolecular arrangement is dictated by hydrogen bonding from the amino functionality and by π–π stacking of the bipyridine rings.

Introduction

Metal complexes of chelating 2,2′-bipyridine (bipy, 1) and secondary terminal or chelating amines are of constant and general interest in metal-coordination chemistry.[1] We have recently engaged into a program to study the coordination behavior of modified 2,2′-bipyridine ligands such as 2,2′-dimethyl-4,4′-bipyrimidine (2),[2] 5,5′-dicyano-2,2′-bipyridine (3),[3] 2,2′-bi-1,6-naphthyridine (4),[4] and modified tris(pyrazolyl)borate ligands.[5] As part of this program we report here the coordinating properties of ambidentate 5,5′-diamino-2,2′-bipyridine (5). The idea behind the use of such ambidentate ligands is to have tetrahedral (6) or octahedral building blocks (7) for supramolecular assemblies based on the chelation of two or three ligands, respectively with an appropriate metal center. The intermolecular connectivity should then be controlled through an NH₂→metal coordination or through hydrogen bonding.[6][7] The amino group on the aromatic ring is a good candidate for hydrogen bonding as has been exploited in the self-assembly of supramolecular entities with 2,4,6-triaminopyrimidine units, for example.[8] The related ligand 2,2′-bipyridine-5,5′-dicarboxylate forms tris(chelate) complexes which are then connected by hydrogen bonding.[9]

Rigid bridging ligands have recently gained considerable interest in the synthesis of (rectangular) two-dimensional network structures.[10] The generation of such frameworks
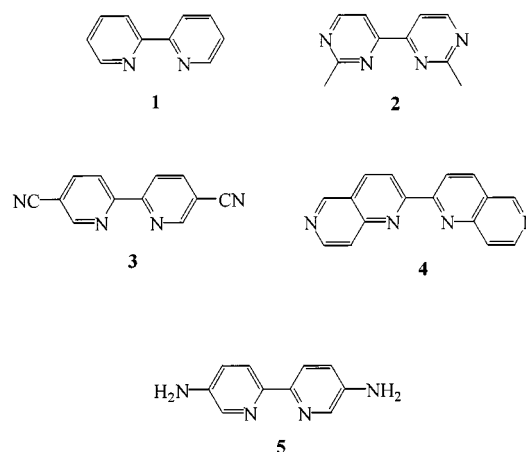
is a promising path in the search for stable microporous metal-organic networks that exhibit reversible guest exchange and possibly selective catalytic activity.[11]

Results and Discussion

Ligand Synthesis

The synthesis of 5 has been achieved according to a route suggested by Whittle (Scheme 1):[12] 5,5′-Dimethyl-2,2′-bipyridine (9) is obtained in medium yield by a Raney nickel catalyzed coupling reaction from β-picoline (8).[13][14] Oxidation with $KMnO_4$ and esterification of the acid then yields the 5,5′-diester 10.[15] Hydrazinolysis of the ester group and hydrazine-azide transformation gives the acyl azide 11. In a Curtius rearrangement this acyl azide is converted by pyrolysis to the isocyanate (R−N=C=O) from which in the presence of ethanol the dicarbamate 12 is derived. Alkaline hydrolysis and sublimation leads to the final

6

7

product **5** in an overall yield of 38% based on 5,5′-dimethyl-2,2′-bipyridine.
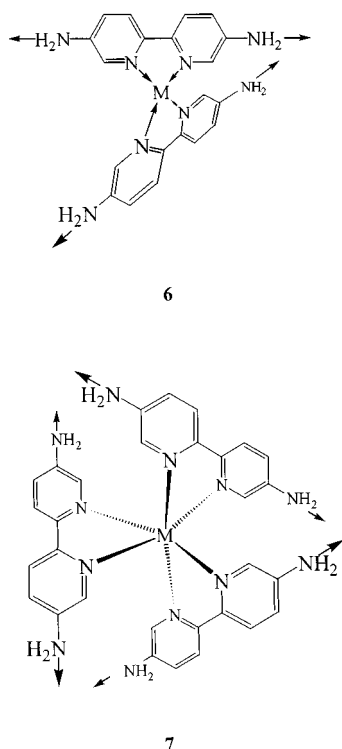
Scheme 1. Synthesis of **5** starting from 3-aminopyridine (**8**)

In order to shorten the synthesis of **5** and to improve the yield, we also tried a new method, namely the coupling of 5-amino-2-chloropyridine (**13**). It was reported in the literature that the coupling of haloaryl or halopyridine compounds in the presence of a catalytic system consisting of $NiCl_2 \times 6\ H_2O$/L/reducing agent could lead to the formation of bipyridine and biaryl derivatives. Such *ni*ckel-containing *c*omplex-*r*educing *ag*ents are generally abbreviated as NiCRALs, L representing PPh_3 or 2,2′-bipyridine. Reducing agents can be zinc[16] or a mixture of sodium hydride and sodium *tert*-butoxide.[17][18] Zerovalent nickel complexes for the coupling of aryl halides were initially introduced by Semmelhack and co-workers.[19]

For the coupling of 5-amino-2-chloropyridine the use of sodium hydride as a reducing agent for the nickel complex

to give the NiCRAL was unsuccesful. The necessary excess of NaH apparently deprotonates the amino function of the pyridine, which then coordinates to the nickel center so that the reaction is slowed down considerably. After 5 d under reaction conditions, the starting compound was still present and only traces of **5** were found. This is remarkable, since under the same conditions 2-amino-3-chloropyridine is coupled to the 2,2′-diamino-3,3′-bipyridine in 44% yield in 17 h.[17]

The use of zinc powder as a reducing agent for the NiC-RAL was eventually successful: A solution of nickel(II) chloride hexahydrate and triphenylphosphane in DMF was reduced with zinc and was subsequently treated with a stoichiometric amount of 5-amino-2-halopyridine. No pyridine compound could be detected anymore after 2−2.5 h and workup yielded the coupling product **5** in over 60% yield (Scheme 2). The starting compound for the coupling reaction, the amino-substituted 2-halopyridine **13b** was obtained from the commercially available 2-chloro-5-nitro-pyridine (**13a**).[20]
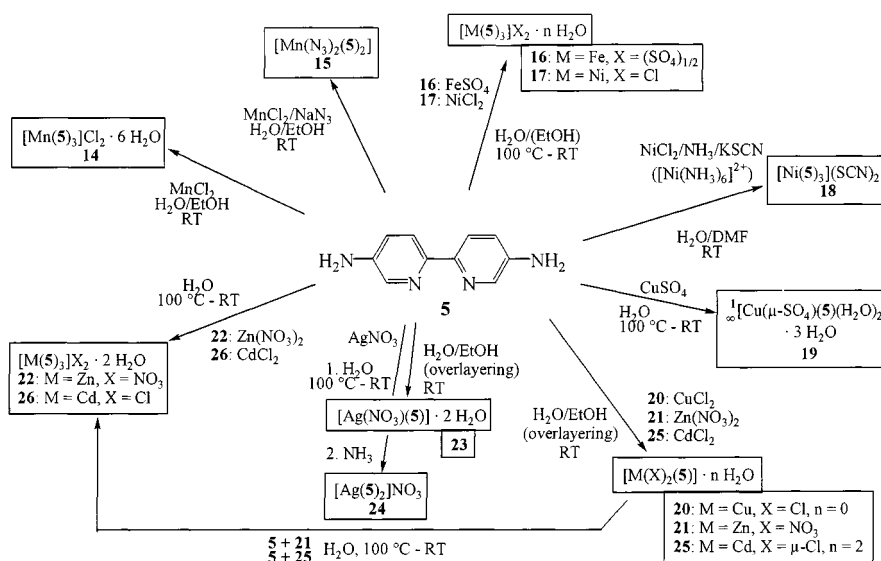

13a   **13b**

5
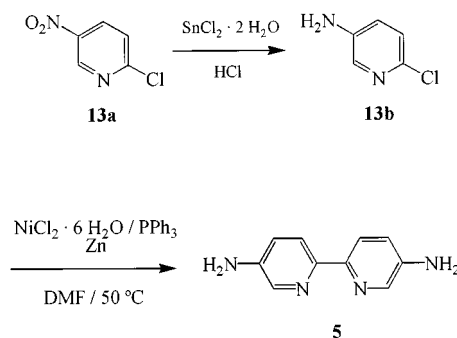
Scheme 2. Synthesis of **5** based on an NiCRAL−catalyzed coupling of 5-amino-2-chloropyridine (**13b**)

Syntheses of Metal Complexes of 5

Different methods were used for the syntheses of metal complexes of **5**. An overview of the prepared metal compounds is provided in Scheme 3.

In the case of the manganese complexes $[Mn(5)_3]Cl_2$ (**14**) and $[Mn(N_3)_2(5)_2]$ (**15**) it was sufficient to combine the reactands in solution and let them stand for some time. For the d^5-high-spin Mn^{2+} ion ligand substitution results only in a small gain of energy because of the theoretically zero ligand field stabilization energy (LFSE). Hence, the thermodynamic driving force for the formation of the manganese chelate complexes from the hexaaquametal ions is small and the reaction proceeds much slower than for iron, nickel and copper which have larger LFSE contributions.[21]

Heating an aqueous suspension or an ethanolic solution of **5** with a solution of the metal salt in water gave upon cooling the tris(5,5′-diamino-2,2′-bipyridine)metal complexes $[M(5)_3]^{2+}$ of iron as the sulfate (**16**), nickel as the chloride (**17**), zinc as the nitrate (**22**), and cadmium as the chloride (**26**). Furthermore, the mono(5,5′-diamino-2,2′-bipyridine)diaqua(μ-sulfato)copper compound **19** and a

$[Mn(N_3)_2(5)_2]$
15

$[M(5)_3]X_2 \cdot n\, H_2O$
16: M = Fe, X = $(SO_4)_{1/2}$
17: M = Ni, X = Cl

$[Mn(5)_3]Cl_2 \cdot 6\, H_2O$
14

MnCl$_2$/NaN$_3$
H$_2$O/EtOH
RT

16: FeSO$_4$
17: NiCl$_2$

H$_2$O/(EtOH)
100 °C - RT

NiCl$_2$/NH$_3$/KSCN
([Ni(NH$_3$)$_6$]$^{2+}$)

$[Ni(5)_3](SCN)_2$
18

MnCl$_2$
H$_2$O/EtOH
RT

H$_2$O
100 °C - RT

H$_2$N —⟨N⟩—⟨N⟩— NH$_2$
5

H$_2$O/DMF
RT

CuSO$_4$
H$_2$O
100 °C - RT

$^{1}_{\infty}[Cu(\mu\text{-}SO_4)(5)(H_2O)_2]$
$\cdot 3\, H_2O$
19

22: Zn(NO$_3$)$_2$
26: CdCl$_2$

$[M(5)_3]X_2 \cdot 2\, H_2O$
22: M = Zn, X = NO$_3$
26: M = Cd, X = Cl

AgNO$_3$
1. H$_2$O
100 °C - RT

H$_2$O/EtOH
(overlayering)
RT

$[Ag(NO_3)(5)] \cdot 2\, H_2O$
23

2. NH$_3$

$[Ag(5)_2]NO_3$
24

H$_2$O/EtOH
(overlayering)
RT

20: CuCl$_2$
21: Zn(NO$_3$)$_2$
25: CdCl$_2$

$[M(X)_2(5)] \cdot n\, H_2O$
20: M = Cu, X = Cl, n = 0
21: M = Zn, X = NO$_3$
25: M = Cd, X = μ-Cl, n = 2

5 + 21
5 + 25 H$_2$O, 100 °C - RT

Scheme 3. The metal complexes of 5,5'-diamino-2,2'-bipyridine (**5**)
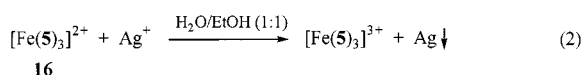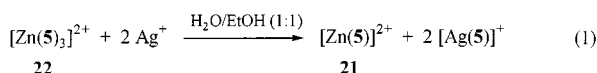
mono(5,5'-diamino-2,2'-bipyridine)silver derivative (see **23**) was obtained by such a hydrothermal reaction. Also [Zn(NO$_3$)$_2$(**5**)] (**21**) and [Cd(μ-Cl)$_2$(**5**)] (**25**) react with two equivalents of **5** under reflux to form the homoleptic tris-(chelate) complexes [Zn(**5**)$_3$](NO$_3$)$_2$ (**22**) and [Cd(**5**)$_3$]Cl$_2$ (**26**), respectively. This observation agrees with the complexation behavior found for 2,2'-bipyridine.[22]

A different synthetic route was chosen for complexes where the coordination sphere was not completely constructed by the diaminobipyridine chelate ligand **5**. Such was the case for the compounds [CuCl$_2$(**5**)] (**20**), [Cd(μ-Cl)$_2$(**5**)] (**24**), and the presumable silver complex [Ag(NO$_3$)(**5**)] (**23**). Here the synthesis was carried out at room temperature mostly by overlayering the aqueous metal salt solution with an ethanolic solution of **5**. To slow down the diffusion of both solvents a layer of ethyl acetate was brought in between the water and the ethanol phase. In three cases it could be shown that the above heteroleptic complexes may be viewed as thermodynamically unstable intermediates along the reaction coordinate to the homoleptic compounds. The 1:1 ligand/metal complexes **21** and **25** react with two equivalents of **5** under reflux to the thermodynamically apparently more stable tris(chelate) complexes [Zn(**5**)$_3$](NO$_3$)$_2$ (**22**) and [Cd(**5**)$_3$]Cl$_2$ (**26**), respectively. A 1:1 ligand/silver complex (as **23**) is initially obtained from the reaction of two equivalents of **5** with one equivalent of Ag$^+$. This complex dissolves in concentrated aqueous ammonia and upon slow evaporation produces the 2:1 ligand/metal complex [Ag(**5**)$_2$]NO$_3$. Such a recrystallization involves formation of the intermediate [Ag(NH$_3$)$_2$]$^+$ complex and slow ligand exchange of the stronger, yet more volatile ammine ligand with **5**.[23] A similar ligand exchange was used in the synthesis of the complex [Ni(**5**)$_3$](SCN)$_2$ (**18**) which was obtained from

mixing the reactands NiCl$_2$, **5**, and KSCN and adding concentrated ammonia, so that the rather stable amminenickel complex [Ni(NH$_3$)$_6$]$^{2+}$ is formed. In addition to the synthetic procedures described in the Experimental Section, the reactions were carried out with different concentrations and different ratios of ligand to metal salt (varied in a wide range between 1:1 and 5:1). In all cases the 3:1 ligand/metal complexes were obtained, though. The deep-red iron complex **16** was formed even in the case of a hundred-fold metal excess. The special stability of iron(II) complexes with 2,2'-bipyridine is well known[24] so that the unsubstituted bipyridine is applied as a test reagent for iron(II).

All of the above metal complexes are insoluble in aliphatic and aromatic solvents and in acetonitrile. The heteroleptic silver and cadmium complexes **23** and **25** are little water- but easily DMSO-soluble. The heteroleptic Cu^{2+} complexes **19** and **20** show a good solubility in water, but they do not dissolve in alcohol or THF. The homoleptic compounds **14** (Mn), **22** (Zn), and **26** (Cd) dissolve well in hot water and DMSO, the tris(chelate)iron and -nickel complexes **16** and **17** are well water-soluble but little in DMSO. Many of the crystalline metal complexes with **5** incorporate water of crystallization which is easily lost upon drying in air, so that the crystals have to be stored in water. The silver complexes **23** and **24** are light-sensitive and have to be stored in the dark.

An attempt was made to use the homoleptic tris(chelate) complexes as building blocks in the reaction with silver nitrate and to achieve the coordination through the amino function (to the silver atom) to give a heterobimetallic coordination polymer. However, a simple ligand exchange was observed when the zinc complex **22** was used (Equation 1) and a redox reaction occurred when the iron complex **16** was employed (Equation 2).

$$[Zn(\mathbf{5})_3]^{2+} + 2\ Ag^+ \xrightarrow{\text{H}_2\text{O/EtOH (1:1)}} [Zn(\mathbf{5})]^{2+} + 2\ [Ag(\mathbf{5})]^+ \qquad (1)$$

22   **21**

$$[Fe(\mathbf{5})_3]^{2+} + Ag^+ \xrightarrow{\text{H}_2\text{O/EtOH (1:1)}} [Fe(\mathbf{5})_3]^{3+} + Ag\!\downarrow \qquad (2)$$

16

Thermal Analyses

Some complexes were studied by thermogravimetry (TG) and differential scanning calorimetry (DSC) to gain information on the amount of the incorporated crystal water, the temperature of water loss and other phase transitions. The TG data on the water loss show good agreement with values from NMR experiments (see Table 1) and fit the elemental analyses data. For **16** and **17** the water content from the X-ray structural analyses is different. This may indicate a varying water content for each single crystal.

After the loss of solvent water, the manganese complex **14** looses a ligand molecule at 290 °C and possibly forms a neutral complex of composition [MnCl₂(**5**)₂], which in turn shows another phase transition at 361 °C. Investigations on solvated tris(2,2′-bipyridine)iron complexes have shown that upon heating the loss of water of crystallization is followed by sequential loss of ligands.[25]

NMR Spectroscopy

Nuclear magnetic resonance spectroscopy is a valuable tool to judge the electronic effects in ligands, including bipyridinemetal chelate complexes.[26] Usually, the d^{10} ions Ag^+ and Cd^{2+} only cause a small down-field shift of the proton signals with respect to those of the free ligand ($\Delta\delta \approx 0.0-0.2$ ppm). A comparison of the chemical shift data for **5** and **22−26** in Table 2 confirms this statement. The small shift is due to the weak Lewis acidity and the small diamagnetic interaction of the ring current with the relatively large cations.[27] This is different for zinc and iron complexes. Since the iron compound **16** was not soluble enough in DMSO, it had to be measured in D_2O and the zinc complex **22** was investigated in both solvents to allow comparison between iron and silver complexes, and the free ligand.

A comparison between the two different solvents for **22** shows the effect of hydrogen bonding from water to the amino functions. This decreases the electron-donating (positive) inductive effect of the amino function to the heterocycle so that especially the signals of the protons in the

Table 2. ¹H-NMR data of diamagnetic metal complexes of **5**
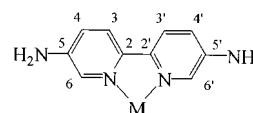
Compound	Solvent	H3, H3′	H4, H4′	H6, H6′
Free ligand **5**	[D₆]DMSO	7.92	6.95	7.84
[Ag(NO₃)(**5**)] (**23**)	[D₆]DMSO	7.92	7.15	7.91
[Ag(**5**)₂]NO₃ (**24**)	[D₆]DMSO	7.91	7.12	7.90
[CdCl₂(**5**)] (**25**)	[D₆]DMSO	7.92	7.14	7.98
[Cd(**5**)₃]Cl₂ (**26**)	[D₆]DMSO	7.90	7.09	7.88
[Zn(**5**)₃](NO₃)₂ (**22**)	[D₆]DMSO	8.08	7.19	7.08
	D₂O	8.43	7.84	7.79
[Fe(**5**)₃]SO₄ (**16**)	D₂O	7.99	7.28	6.85

4- and 6-position experience a low-field shift compared to signals in DMSO. The significant high-field shift of $0.8-1$ ppm of the signal of the proton in 6-position or α to the metal center in **22**/DMSO and **16**/D_2O versus the silver and cadmium complexes is due to the smaller ionic radii of the zinc and iron metal centers. This improves the diamagnetic interaction of the metal center with the ring current.[22][27]

The trends in the shifts in carbon-13 spectroscopy are less straightforward. The signals of the carbon atoms 2, 3, and 6 show only little chemical-shift difference to those of the free ligand (-0.5 to $+0.8$ ppm), the C4 signal experiences a slight down-field shift (1 to 7 ppm) and the C5 signal an up-field shift (2.8 to 4.2 ppm). These trends stem from two superimposing effects: The negative inductive effect of the coordinated metal ion leads in 2- and 6- (*ortho*) position to the nitrogen atom to a down-field shift and to a lesser extent also in the 4- (*para*) position. The interaction of the paired metal d electrons with the diamagnetic ring current, on the other hand, enhances the shielding and consequently induces an upfield shift, which weakens with increasing distance from the metal center.[27][28]

The ligand effect on a metal center was studied with the help of ¹¹³Cd-NMR-spectroscopy. The Cd^II ion has a rather high relaxation time of $0.1-50$ s. Labile complexes which experience rapid ligand exchange, including aqua ligands, then give a broad time-averaged signal. In the building block [Cd(μ-Cl)₂(**5**)] of the heteroleptic complex **25**, the coordination sphere can be concluded by aqua ligands so that the species [CdCl₂(**5**)(H₂O)] and [CdCl₂(**5**)(H₂O)₂] also exist in solution with a rapid interchange among them.[29][30]

Table 1. Thermogravimetic data on the crystal water content in **14**, **16**, and **17**

Compound	Temperature for H₂O loss [°C]	Mass loss [mass%]	ΔH [kJ/g]	Water content [1/formula unit]		
				from TG	from NMR	from X-ray
[Mn(**5**)₃]Cl₂ × 6 H₂O (**14**)	101−150	14.3	34.6	6.3	6.5	−
[Fe(**5**)₃]SO₄ × 6 H₂O (**16**)	162−166	14.1	59.9	6.5	−[a]	9.0
[Ni(**5**)₃]Cl₂ × 6 H₂O (**17**)	145−168	12.3	51.6	5.6	6.0	2.5

[a] Due to the low solubility in [D₆]DMSO the water content could not be verified by NMR.

Hence, the signal for **25** was very broad and could not be clearly assigned. Whereas the tris(chelate) complex **26** gave a rather narrow singlet, which is indicative of the stable nature of $[Cd(\mathbf{5})_3]^{2+}$ in solution. The chemical shift of $\delta = 253$ for **26** [versus 2 M $Cd(ClO_4)_2$ as a standard] falls right in the range observed for other tris(bipyridine) and tris(phenanthroline) complexes: $[Cd(bipy)_3](ClO_4)_2$ ($\delta = 243$), $[Cd(4,4'-Me_2bipy)_3](ClO_4)_2$ ($\delta = 254$), and $[Cd(phen)_3]ClO_4)_2$ ($\delta = 254$ ppm) [all against 0.1 M $Cd(ClO_4)_2$ solution].[29]

Mößbauer Spectroscopy

The iron complex **16** is an exception with respect to its thermodynamic stability in the series of the analogous $[M(\mathbf{5})_3]^{2+}$ derivatives. It forms directly even at high metal excess. A possible explanation is the 3d^6 low-spin configuration of the Fe^{II} ion which possesses a maximal ligand field stabilization energy.[31] Some bipyridineiron(II) complexes are known, e.g. $[Fe(bipy)_3](BF_4)_2 \times 2$ H_2O[32][33] or $[Fe(3,3'-Me_2-bipy)_3](ClO_4)_2$[34] which exhibit a thermally induced low-spin to high-spin crossover. Such a spin crossover changes the spin state from singlet-$^1A_{1g}$ to quintuplet-$^5T_{2g}$ and as a consequence leads to an increase in ligand−metal bond length.[35] Mößbauer spectroscopy allows to discern the spin state of the iron complex. For $[Fe(\mathbf{5})_3]SO_4$ (**16**) in the solid state a pronounced doublet with an isomer shift $\delta(\alpha\text{-Fe}) = 0.30$ mm/s (at 293 K) and a half-width Γ of 0.25 mm/s was found. The quadrupole splitting ΔE_Q was 0.27 mm/s. These values are typical for tris(2,2'-bipyridine) complexes of iron in the low-spin state. The isomer shifts measured, for example, for $[Fe(bipy)_3](ClO_4)_2$, $[Fe(bipy)_3]Cl_2$, and $[Fe(bipy)_3]SO_4$ are 0.30, 0.33, and 0.24 mm/s, respectively.[25,33,36] The small quadrupole splitting in **16** indicates at the most a weak distortion from the octahedral Fe−N$_6$ coordination geometry. The DSC data for **16** exclude the existence of a thermally induced spin transition up to the decomposition temperature of 350°C, because no reversible phase transition could be observed.[5][37] Another indication along the same lines is the deep-red color of **16** which stems from the $^1A_{1g} \rightarrow {}^1T_{1g}$ d-d transition. Upon heating, this color does not fade as would be expected from a spin crossover, because the smaller d-d splitting in the high-spin state shifts the absorption from the visible into the infrared regime.[5][38] Both negative indicators for a spin crossover behavior precluded a temperature-variable Mößbauer study.

Infrared Spectroscopy

Metal complexes with 2,2'-bipyridine ligands were the subject of intense IR-spectroscopical investigations.[39−41] All bands are now clearly assigned. Some of the many ring vibrations are sensitive to metal coordination and experience an hypsochromic shift (to higher wavenumbers or energy) of 10 to 20 wavenumbers.[40] The influence of the metal coordination on the vibrations of the amino function has been elucidated with the 2- and 3-aminopyridine ligand.[42][43] The in-plane ring-stretch vibrations of **5** are found at 1568, 1478 and 656 cm^{-1}.[44] The first two show in all metal complexes the aforementioned hypsochromic shift to 1579−1590 cm^{-1} and 1486−1497 cm^{-1}, respectively. The band at 656 cm^{-1} either remains almost unshifted (in **15**, **16**, **17**, **18**, **22**, **24**, and **25**) or is split into two bands (as in **14**, **19**, **23**, and **26**). Similarly, the corresponding band in $[Mn(bipy)_3](ClO_4)_2$ is split.[40][41] The explanation is sought in a substantial twist (over 10°) of the pyridine ring planes around the connecting C2−C2′ bond away from the almost coplanar to a twisted *cis* configuration (**27**).

coplanar cis configuration   twisted cis configuration

27
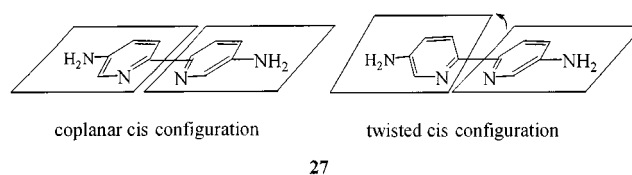
To the extent of a few degrees the ring planes in a bipyridine pair are always twisted (see below).[45] An X-ray structure analysis of $[Mn(bipy)_3](ClO_4)_2$ confirmed the substantial twist, the dihedral angles between each pair of pyridine rings in all three bipyridine ligands lay between 13 and 25°.[46]

The structures collected here do not reveal a substantial twist in any case. The dihdral angles between the pyridine ring planes were 9.7° in **15**, 5.3, 5.7, and 11.3° in **18**, 3.3° in **19**, 2.3° in **20**, 5.2, 8.9, and 9.1° in **22**, and 0.1° in **25**. This finding coincides with the non-splitting of the band at around 656 cm^{-1} but does not agree with the splitting found for **19**. Hence, the IR analysis with respect to a twisted configuration should be applied with caution.

From aqueous solutions the ligand **5** crystallizes as the monohydrate. The IR spectrum of $\mathbf{5} \times H_2O$ then shows two sharp bands at 3425 and 3340 cm^{-1}, which are assigned to the symmetric and asymmetric NH stretch. Three additional and broader bands at 3376, 3315, and 3205 cm^{-1} are due to the formation of amino hydrogen bonds to the water oxygen atom. The NH deformation is found at 1632 cm^{-1}. In all metal complexes the position of this bending vibration remains rather unchanged, different to what would be expected in case of amino−metal complexation.[42]

X-ray Structural Studies

Generally, all of the metal complexes of **5** which are structurally elucidated here show a bipyridine−metal coordination of the potentially ambidentate diaminobipyridine ligand. The amino functionality was never involved in metal coordination, yet, could play a substantial role in hydrogen bonding (see below). Specific distances and angles and some figures for the hydrogen bonding networks which are not given here, can be found in the supporting information. The specific structures are described in some more detail in the following.
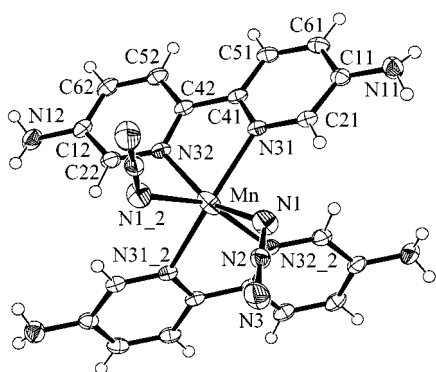
Figure 1. Molecular structure of [Mn(N₃)₂(**5**)₂] (**15**); selected distances [Å] and angles [°]: Mn−N1 2.211(1), Mn−N31 2.265(1), Mn−N32 2.286(1), N1−N2 1.171(2), N2−N3 1.168(2); N1−Mn−N1#2 86.58(8), N1−Mn−N31#2 113.66(4), N1−Mn−N31 89.19(4), N31−Mn−N31#2 149.14(5), N1−Mn−N32 154.51(5), N1−Mn−N32#2 86.07(5), N31#2−Mn−N32#2 71.61(4), N31−Mn−N32#2 90.61(4), N32−Mn−N32#2 110.09(6), N1−N2−N3 178.1(1) (symmetry equivalent position #2 = 0.5 − *x*, *y*, −*z*)

[Mn(N₃)₂(5)₂] (15)

Figure 1 illustrates the structure of this molecular complex. The two azide ligands are *cis*-coordinated, terminally bound and do not bridge between metal centers. The bonding mode is not unusual for coordinated azides.[47] The pseudooctahedral structure of **15** is similar to *cis*-[Mn(NCS)₂(bipy)₂].[48] The M−N(bipy) bond lengths *trans* to the azide (or NCS) ligand show some lengthening. The crystal structure is stabilized by stacking interactions involving bipyridine ligands of adjacent molecules (π−π contacts down to 3.2 Å). Intermolecular hydrogen bonding from the amino functions to the N3 atom of the azide ligand is observed.

[Fe(5)₃]SO₄ × 9 H₂O (16)

The tris(chelate) structure (cf. Figure 3) of the [Fe(**5**)₃]²⁺ moiety is unremarkable (Table 3). Recent examples of [Fe(bipy)₃]²⁺ complexes include the counterions [Fe(NO)₂Cl₂]⁻,[49] [Fe₂OCl₆]²⁻,[50] [Fe₂(ox)₃]²⁻,[51] and
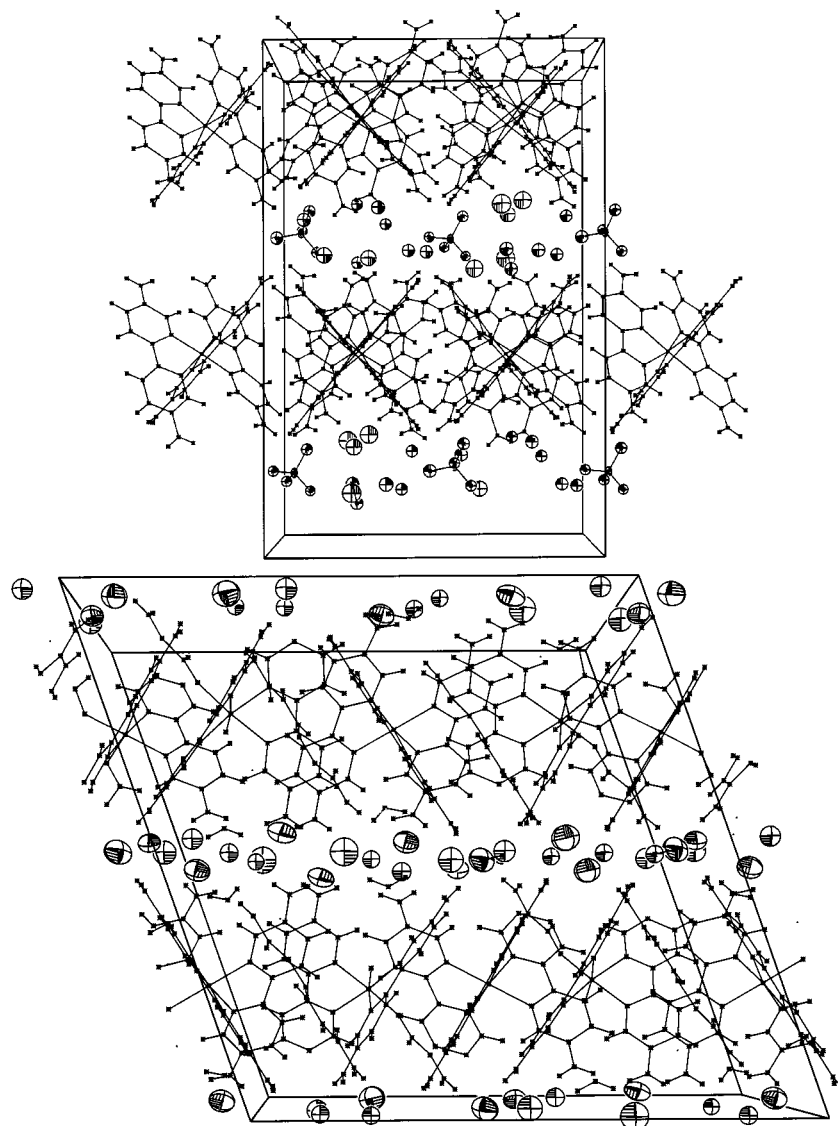
Figure 2. Layer arrangement of the [M(**5**)₃]²⁺ cations and the anions (SO₄²⁻ or Cl⁻) together with the water of crystallization in the structures of (a, top) [Fe(**5**)₃]SO₄ × 9 H₂O (**16**) and (b, bottom) [Ni(**5**)₃]Cl₂ × 2.5 H₂O (**17**); view along *a* (a) and *b* (b)

[MC(ox)$_3$]$^{2-}$,[52][53] (ox = oxalate, M = Ag, Na, Li). We just note that **16** is constructed from alternating layers of the tris(chelate) cations and layers of the sulfate anions together with the water of crystallization (Figure 2a). The interaction between the layers occurs through hydrogen bonding from the amino group to the oxygen centers.

[Ni(5)$_3$]Cl$_2$ × 2.5 H$_2$O (17) and [Ni(5)$_3$](SCN)$_2$ (18)

The tris(chelate) structure around the nickel centers (Figure 3, Table 3) is common in a sizable number of tris(bipyridine)metal complexes which are described in the literature. Recent examples are [Ni(bipy)$_3$][Mn$_2$(ox)$_3$],[53] [Ni(bipy)$_3$]-NaAl(ox)$_3$],[54] [Ni(bipy)$_3$][Ni(CN)$_4$] × bipy × 6 H$_2$O,[55] and [Ni(bipy)$_3$]$_2$[Ag(CN)$_2$]$_3$Cl × 9 H$_2$O.[56] The structure of **17** contains an analogous layer arrangement as seen before in **16** (Figure 2b). Noteworthy in **18** is the hydrogen bonding from the amino groups to both the sulfur and the nitrogen end of the SCN anions.
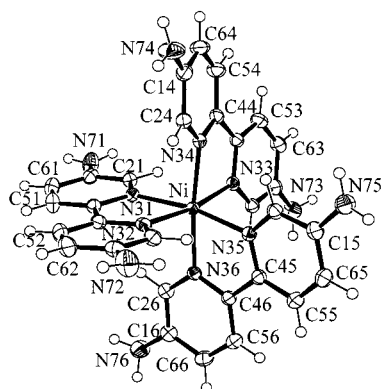

Figure 3. Exemplified view of the molecular structure of the tris(chelate)metal cations in [Fe(**5**)$_3$]SO$_4$ × 9 H$_2$O (**16**), [Ni(**5**)$_3$]Cl$_2$ × 2.5 H$_2$O (**17**), [Ni(**5**)$_3$](SCN)$_2$ (**18**, shown here), and in [Zn(**5**)$_3$](NO$_3$)$_2$ (**22**); selected distances and angles are given in Table 3

$^1_\infty$[Cu(μ-SO$_4$)(5)(H$_2$O)$_2$] × 3 H$_2$O (19)

Figure 4a shows a section of the 1-dimensional coordination polymer and Figure 4b displays the stabilizing π−π interaction (about 3.4 Å)[57] of adjacent strands. The chains
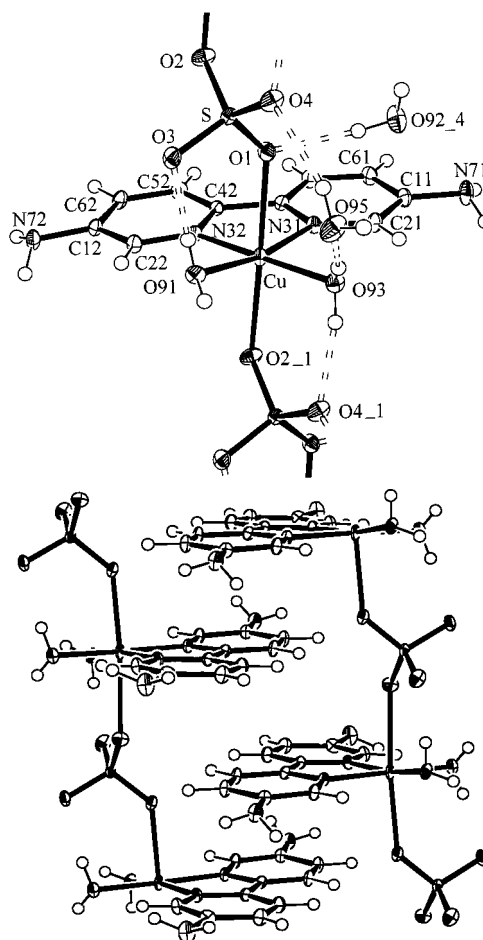

Figure 4. (a, top) Section of the one-dimensional coordination polymer $^1_\infty$[Cu(μ-SO$_4$)(**5**)(H$_2$O)$_2$] × 3 H$_2$O (**19**) indicating also part of the hydrogen bonding network with two water molecules of crystallization; selected distances [Å] and angles [°]: Cu−N31 2.010(2), Cu−N32 1.992(2), Cu−O91 2.006(2), Cu−O93 1.993(2), Cu−O1 2.468(2), Cu−O2#1 2.311(2); N32−Cu−O93 175.08(6), O91−Cu−N31 168.89(6), O1−Cu−O2#1 173.73(6), O93−Cu−O91 92.61(6), N32−Cu−N31 82.10(6), O1−Cu−N31 86.54(6), O1−Cu−O91 84.38(6), O91−Cu−O2#1 90.03(6), N31−Cu−O2 99.33(5), other angles between *cis*-positioned atoms range from 88.3 and 93.6° (symmetry equivalent position #1 = x − 1, y, z; #4 = x − 0.5, −y + 0.5, z − 0.5); (b, bottom) π-π stacking of neighboring strands, running along *a*

Table 3. Selected bond lengths and angles in the tris(chelate)metal complexes [M(**5**)$_3$]$^{2+}$

	[Fe(**5**)$_3$]$^{2+}$ (in **16**)[a]	[Ni(**5**)$_3$]$^{2+}$ (in **17**)[a]	[Ni(**5**)$_3$]$^{2+}$ (in **18**)	[Zn(**5**)$_3$]$^{2+}$ (in **22**)
M−N range [Å]	1.941(9)−1.995(9)	2.075(4)−2.095(3)	2.0742(15)−2.1152(16)	2.145(3)−2.212(3)
M−N average [Å]	1.968	2.084	2.094	2.167
N−M−N chelate bite angles [°]	81.9(4) (3 ×), 82.0(4), 82.2(3), 82.3(4)	78.9(2), 79.0(2), 79.1(2) (2 ×), 79.3(2), 79.4(2)	78.83(6), 79.04(6), 79.07(6)	76.4(1), 77.6(1), 77.9(1)
N−M−N *cis*, except chelate, range [°]	88.7(4)−96.9(4)	90.4(1)−96.8(1)	91.32(6)−97.26(6)	92.6(1)−97.1(1)
average N−M−N *cis*, except chelate [°]	92.7	93.8	93.89	94.6
N−M−N *trans* [°]	172.7(4), 173.2(4), 173.9(4), 175.1(4), 175.2(4), 175.6(4)	168.1(2), 169.4(1), 170.1(1), 170.5(2), 173.7 (2), 173.8(1)	169.05(6), 170.36(5), 173.13(6)	166.6(1), 167.3(1), 169.6(1)

[a] Two symmetically independent molecules in the unit cell.

C. Janiak, S. Deblon, H.-P. Wu, M. J. Kolm, P. Klüfers, H. Piotrowski, P. Mayer

are formed through the bridging action of the sulfato ligand, two of which are arranged *trans* around the copper center with Jahn−Teller-elongated Cu−O contacts. The aqua and sulfato ligands on the metal center and the water molecules of crystallization form a three-dimensional hydrogen-bonding network surrounding the π-interacting double strands from Figure 4.

[CuCl₂(5)] (20)

The structure of this molecular complex is displayed in Figure 5. The copper atom is four-coordinate with a coordination polyhedron between square-planar and tetrahedral. The dihedral angle between the plane of the five-membered chelate ring and the Cl−Cu−Cl plane is 41.1°. In the complex (3-amino-6,6′-dimethyl-2,2′-bipyridine)dichlorocopper(II) a (Jahn−Teller-)compressed tetrahedral structure is found since the methyl groups *ortho* to the coordinating nitrogen atom apparently prevent a more planar ligand arrangement.[58] An approximately square-planar coordination around Cu is observed in (2,2′-bipyridine-3,3′-dicarboxylic acid)dichlorocopper(II) monohydrate.[59] However, weak intermolecular interactions with a Cl atom (3.117 Å) and an O atom (2.678 Å away) on adjacent molecules complete an octahedral donor arrangement around the metal center. In **20** no such intermolecular interactions can be found; the next chlorine contact to a neighboring molecule is 5.28 Å. The absence of bridging chlorine atoms in **20** is unusual as in the related compounds dichloro(4,4′-dimethyl-2,2′-bipyridine)copper(II) hemihydrate[60] and in dichloro(2,2′-bipyridine)copper(II)[61] such intermolecular interactions are present leading to five- and six-coordinate copper centers in dimeric and polymeric structures, respectively. The chlorine atoms in **20** are involved in hydrogen bonding to the amino group (H···Cl 2.799 and 2.858 Å, see Figure 8a), yet, it is unclear if this is sufficient to prevent coordination to the copper atom (see below). That such intermolecular interaction are feasable is demonstrated with the structure of $^{1}_{\infty}$[Cd(μ-Cl)₂(5)] × 2 H₂O (**25**). The packing of the molecules of **20** (π−π distances around 3.4 Å) is discussed in combination with the related structure of **25** below.
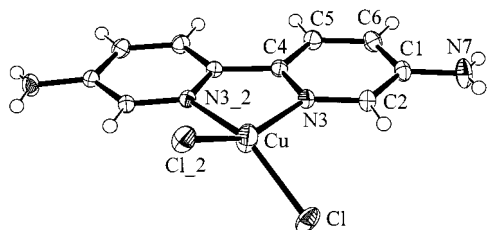

Figure 5. Molecular structure of [CuCl₂(**5**)] (**20**); selected distances [Å] and angles [°]: Cu−N3 1.981(1), Cu−Cl 2.2346(4); N3−Cu−N3#2 82.28(8), N3−Cu−Cl 97.41(4), N3−Cu−Cl#2 150.80(4), Cl−Cu−Cl#2 96.61(2) (symmetry equivalent position #2 = −x + 1, y, −z + 0.5)

[Zn(5)₃](NO₃)₂ × 2 H₂O (22)

The unspectacular tris(chelate) structure is again found in **22** (cf. Figure 3, Table 3). We refer to [Zn(bipy)₃](SCN)₂ × 7 H₂O[62] and to the various structures of [Zn(bipy)₃]-ClO₄)₂[63] as recent examples. Of more interest is an extended, two-dimensional hydrogen-bonded network formed by the nitrate anions, the water molecules of crystallization and the amino functions of the bipyridine ligands (Figure 6). These hydrogen-bonded grids separate and sandwich the layers build from the tris(chelate) complex molecules (and vice versa). Within such a network the amino groups hydrogen-bond either to one (N56) or two nitrate ions (N53, N54, N55) or bridge with their hydrogen atoms between a nitrate anion and a water molecule (N52) or between two water molecules (N51). One of the hydrogen atoms from N54 thereby forms a 3-center or bifurcated bridge to two oxygen atoms (O1 and O2) of a nitrate ion. One of the water molecules (O92) bridges between two nitrate anions and accepts a hydrogen bond from the other solvent water (O91). The latter forms hydrogen bonds between a nitrate ion and a water molecule and the oxygen atom accepts three hydrogen bonds from amino groups to become five-coordinate. Each of the nitrate ions is anchored by five or six hydrogen bonds, four of which are derived from the amino groups and the remaining one or two from water molecules. Figure 6 illustrates the hydrogen-bonded network and Table 4 provides further details.
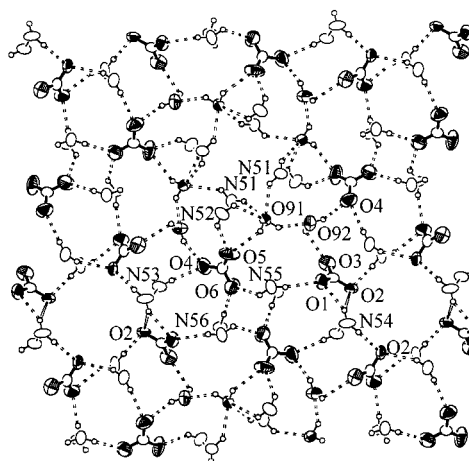
Figure 6. Two-dimensional hydrogen bonding network in [Zn(**5**)₃](NO₃)₂ (**22**) in the *ab* plane; the nitrogen atoms of the amino groups are drawn as empty ellipsoids only; due to space requirements only part of the atom positions are labelled and symmetry operations are not shown

$^{1}_{\infty}$[Cd(μ-Cl)₂(5)] × 2 H₂O (25)

The building block for this one-dimensional coordination polymer is drawn in Figure 7a. At first sight, the structure is similar to the copper complex **20**. The dihedral angle between the plane of the five-membered chelate ring and the Cl−Cd−Cl plane is 17.8°. However, unlike **20** the cadmium compound forms 1D strands (Figure 7b). Polymer formation is based on the bridging action of the chloro ligands as is evident from Figure 7b. The distorted octahedral coordination sphere of cadmium thus consists of the two bipyridine nitrogen atoms and four bridging chlorine atoms. The cadmium−chlorine (2.561, 2.781 Å) and cadmium−cad-

Table 4. Hydrogen bonding interactions in [Zn(**5**)₃](NO₃)₂ × 2 H₂O (**22**); symmetry equivalent positions: #4 = −y − 0.25, −x + 0.75, z − 0.25; #6 = −x + 1, −y + 0.5, z; #7 = x − 0.25, −y + 0.25, z − 0.25; #9 = −x + 1, −y + 1, −z; #12 = −y + 1.25, x + 0.25, −z + 0.25; #14 = x, y + 0.5, −z; #15 = y − 0.25, −x + 1.25, −z + 0.25

D−H···A	D−H [Å]	H···A [Å]	D···A [Å]	D−H···A [°]
N51−H51B···O91	0.880(4)	2.258(4)	3.048(6)	149.3(3)
N51−H51A···O91#15	0.879(4)	2.326(4)	3.051(5)	139.8(3)
N52−H52A···O91#4	0.880(5)	2.445(4)	3.038(6)	125.1(3)
N52−H52B···O5#4	0.881(5)	2.302(5)	3.061(7)	144.4(3)
N53−H53A···O2#6	0.882(4)	2.128(4)	2.923(5)	149.7(3)
N53−H53B···O4	0.879(5)	2.069(5)	2.889(7)	154.9(3)
N54−H54A···O1#7	0.881(4)	2.326(4)	3.148(6)	155.3(4)
N54−H54A···O2#7	0.881(4)	2.456(5)	3.217(6)	144.9(3)
N54−H54B···O2#9	0.879(5)	2.177(4)	3.029(6)	163.2(3)
N55−H55A···O6#15	0.880(4)	2.457(6)	3.114(7)	131.9(3)
N55−H55B···O1#15	0.878(4)	2.146(4)	3.004(5)	165.5(3)
N56−H56A···O6#14	0.880(4)	2.137(6)	3.010(7)	171.5(4)
O91−H911···O92	0.908(19)	1.881(19)	2.657(7)	142.1(19)
O91−H912···O5	0.89(2)	2.34(2)	2.901(6)	120.9(19)
O92−H921···O3	0.83(4)	2.31(5)	2.742(8)	113(3)
O92−H922···O4#12	0.82(3)	2.36(4)	2.892(8)	123(4)

Figure 7. (a, top) Building block for the one-dimensional coordination polymer ¹∞[Cd(μ-Cl)₂(**5**)] × 2 H₂O (**25**) and (b, bottom) partial packing diagram which shows the formation of one-dimensional strands; the water molecules of crystallization have been omitted for clarity; selected distances [Å] and angles [°]: Cd−N1 2.332(8), Cd−Cl,Cl#3 2.561(8), Cd−Cl#5,7 2.78(1); N1−Cd−N1#3 70.2(4), N1−Cd−Cl 159.6(11), N1−Cd−Cl#7 96.5(2), Cl−Cd−Cl#3 103.2(3), N1#3−Cd−Cl 94.5(3), N1#3−Cd−Cl#7 85.8(2), Cl−Cd−Cl#7 95.7(3), Cl#3−Cd−Cl#7 82.5(3) Cl#7−Cd−Cl#5 177.17(4) (symmetry transformations: #3 = −x, y, −z + 0.5; #5 = −x, −y, −z; #7 = x, −y, z + 0.5)

mium (4.04 Å) distances found here are typical for chlorobridged cadmium compounds.[64] The amino groups are not involved in metal coordination but take part in the hydrogen bonding network build up by the water of crystallization.

The packing and strand formation in **25** by chlorine bridging can be compared to the packing of the molecular complexes of **20**. Figure 8 contrasts similar views of the unit cells of both compounds. It can be seen that the bipyridine π−π stacking (both from 3.4 Å on in **20** and in **25**)[57] is an important motif to control the intermolecular arrangement, as was also pointed out in Figure 4 for the copper complex **19**; π strands are formed with the MCl₂ moieties alternatingly facing to the left and right of these stacks. These π interactions may be more important in **20** than in **25**, since
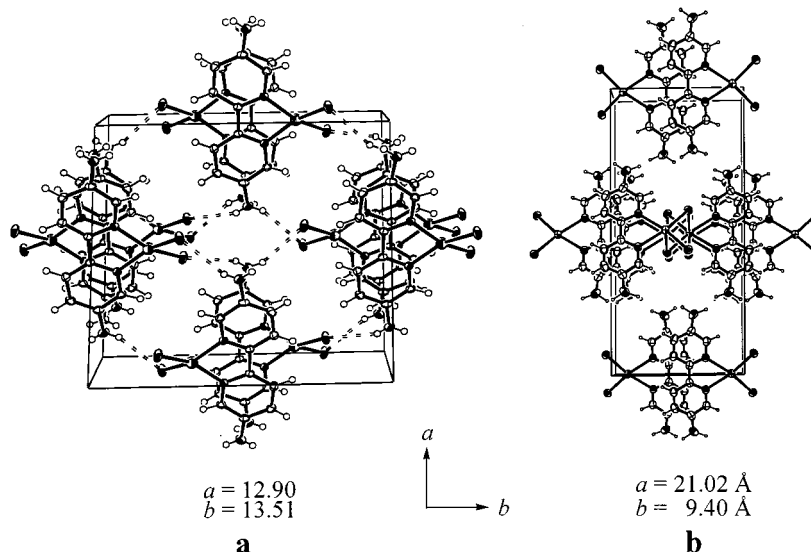
the ring overlap is larger in the copper than in the cadmium compound. On the basis of the molecular copper complex in Figure 8a, the metal−chlorine bridging in **25** (Figure 8b) can be developed by stretching the a axis and shortening the b axis. Cadmium−chlorine bridging can then occur along b between the CdCl₂ moieties which face each other. Starting from the complete ring overlap in **20** the bridging in **25** is enhanced at the cost of the bipyridine π overlap by moving the (bipy)CdCl₂ moieties to the left and right in the b direction, so that the ring overlap is greatly diminished.

a = 12.90
b = 13.51

a

a = 21.02 Å
b = 9.40 Å

b

Figure 8. (a, left) unit cell of [CuCl₂(**5**)] (**20**) and (b, right) unit cell of ¹∞[Cd(μ-Cl)₂(**5**)] × 2 H₂O (**25**), both viewed approximately along c, to compare the relationship between the unbridged and chlorine-bridged packing; hydrogen−chlorine bonding is indicated in **20**; the water molecules of crystallization in **25** have been omitted for clarity
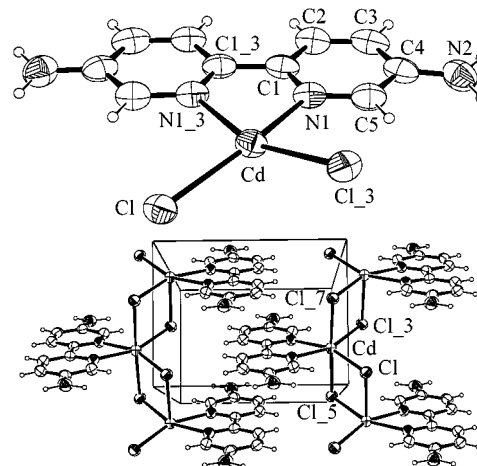
Conclusions

The expectation that the potentially ambidentate group 5,5′-diamino-2,2′-bipyridine (**5**) could function as a bridging and/or chelating bi- to tetradentate ligand in the coordination of transition metals has not been fulfilled. This may be traced to the delocalization of the amine lone-pair into the electron-deficient pyridine ring. The structural studies showed a well-developed coplanarity of the amino group with the aromatic ring. However, the amino function takes part in hydrogen bonding to the anions and to incorporated water molecules of crystallization. From this a two- to three-dimensional hydrogen-bonding network was created which was one of the factors in the packing of the molecular or extended ligand−metal complexes. The other key factor responsible for the supramolecular arrangement of the 5,5′-diamino-2,2′-bipyridine−metal entities is a face-to-face π−π stacking interaction between bipyridine ligands of neighboring ligand−metal fragments. The importance of such a π−π stabilization[57] for the ligand−metal packing has also been elucidated in the structures of the metal complexes with 2,2′-dimethyl-4,4′-bipyrimidine (**2**),[2] 5,5′-dicyano-2,2′-bipyridine (**3**),[3] and 2,2′-bi-1,6-naphthyridine (**4**).[4] These last three ligands also exhibit the sought for bridging and/or chelating bi- to tetradentate metal coordination.

Experimental Section

General: NMR: Bruker ARX 200 (200.1 MHz for ^{1}H, 50.3 MHz for ^{13}C) or Varian O-300 (300.0 MHz for ^{1}H, 75.4 MHz for ^{13}C); calibrated against the solvent signal ([D$_6$]DMSO: ^{1}H NMR: δ = 2.53; ^{13}C NMR: δ = 39.5; CDCl$_3$: ^{1}H NMR: δ = 7.26; ^{13}C NMR: δ = 77.0; C$_6$D$_6$: ^{1}H NMR: δ = 7.19; ^{13}C NMR: δ = 128.0). − Thermogravimetric analyses: simultaneous thermoanalysis apparatus STA 429 from Netsch. − IR spectra: Perkin−Elmer 783 infrared spectrophotometer as KBr disks or as Nujol mulls. − Mass spectra: GC/MS Finnigan MAT in solid-probe EI mode at an ionization energy of 70 eV. − Elemental analyses: Perkin−Elmer elemental analyzer E 240 C. − Commercial triphenylphosphane was dried for 24 h in vacuo at 50°C. Distilled water was carefully degassed prior to use. Dimethyl formamide (DMF) was of technical grade and was fractionally distilled with 10 vol-% of toluene and 2 vol-% of water. This prepurified DMF was stirred for 2 h over CaH$_2$ under argon and then distilled under vacuum. 5-Amino-2-chloropyridine (**13b**) was prepared as described in ref.[20] from 2-chloro-5-nitropyridine (**13a**) in 92% yield.

Synthesis of 5 from 3-Methylpyridine (8) (Scheme 1)

5,5′-Dimethyl-2,2′-bipyridine (9): *CAUTION:* Dry Raney nickel is highly pyrophoric! In a 250-mL three-necked flask 20 g of nickel/aluminum alloy were added under inert gas and ice-cooling in portions within 30 min to a solution of 25.6 g (0.64 mol) of NaOH in 100 mL of water. The temperature increased quickly to 80°C. After complete addition, stirring was continued at 80°C for 1 h. Then 100 mL of water was added and the solution was decanted from the Raney nickel. The latter was washed 20 times with 100 mL of H$_2$O each, which was decanted each time after 2 min of stirring. Afterwards the three-necked flask was fitted with a reflux condenser and a dropping funnel. The remaining water was first removed with a water aspirator at 60°C, eventually the Raney nickel

was dried at 0.05 mbar at 80°C for 3 h. Then, 30 mL (0.29 mol) of 3-methylpyridine (**8**) was slowly added dropwise under ice-cooling and the reaction mixture was kept for 5 d at an oil-bath temperature of 180°C. The product was filtered hot through a D3 frit and the Raney nickel residue washed twice with hot toluene. (The Raney nickel was slowly dissolved with water, medium concentrated HCl and conc. HNO$_3$.) The filtrate was freed from the starting compound and toluene by vacuum distillation. The product was sublimed twice and obtained in colorless needle-shaped crystals (yield 9.5 g, 36%; ref.[13][14] 17%). − The procedure could easily be scaled up six-fold: From 125 g of nickel/aluminum alloy, 160 g of NaOH, two times 600 mL of degassed water and 188 mL of 3-methyl-pyridine was obtained 55 g of **9** (31%). A 2-l flask was used as the reaction vessel and the reaction mixture was kept for 4 d at 180°C. The Raney nickel residue was washed three times with 80 mL of hot toluene, each. − M.p. 114°C (ref.[13] 114.5−115°C. − ^{1}H NMR (CDCl$_3$): δ = 8.41 (d, 2 H, J = 1.5 H, H6, H6′), 8.17 (d, 2 H, J = 9.0 Hz, H4, H4′), 7.52 (dd, 2 H, J_1 = 8.0 Hz, J_2 = 2.0 Hz, H3, H3′), 2.29 (s, 6 H, CH$_3$). − ^{13}C NMR (CDCl$_3$): δ = 153.7 (C2, C2′), 149.5 (C6, C6′), 137.3 (C4, C′), 132.9 (C5, C5′), 120.2 (C3, C3′), 18.2 (methyl-C). − The numbering for the NMR notation for **5, 9−12** is as in Scheme 4.
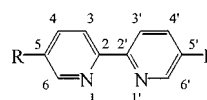
Scheme 4. Numbering scheme for bipyridines

Diethyl 2,2′-Bipyridine-5,5′-dicarboxylate (10): 9.45 g (51 mmol) of **9** were added to a solution of 50.0 g (317 mmol) of KMnO$_4$ in 600 mL of water. The mixture was refluxed until decolorization had occurred. The solution was filtered from precipitated MnO$_2$ and the filtrate acidified with half-concentrated HCl. A fine colorless powder of 2,2′-bipyridine-5,5′-dicarboxylic acid precipitated. This intermediate (M.p. > 280°C) was separated by filtration, dried in vacuo and suspended in 200 mL of dried ethanol. After careful addition of 50 mL of conc. H$_2$SO$_4$, the reaction mixture was refluxed for 16 h to give a clear solution. The warm solution was poured onto ice. The hitherto obtained precipitate was filtered, washed several times with water, dried and recrystallized from ethanol to give **10** as colorless needles (yield 9.8 g, 64%). − M.p. 145°C (ref.[12]: 147°C) − ^{1}H NMR ([D$_6$]DMSO): δ = 9.18 (d, 2 H, J = 2.5 Hz, H6, H6′), 8.54 (dd, 2 H, J_1 = 8.6 Hz, J_2 = 2.5 Hz, H4, H4′), 8.44 (d, 2 H, J = 8.6 Hz, H3, H3′), 4.38 (q, 4 H, J = 7.1 Hz, OCH$_2$), 1.36 (t, 6 H, J = 7.1 Hz, CH$_3$). − ^{13}C NMR (CDCl$_3$): δ = 164.2 (*C*OOEt), 157.3 (C2, C2′), 149.8 (C6, C6′), 137.9 (C4, C4′), 126.2 (C5, C5′), 121.0 (C3, C3′), 61.0 (OCH$_2$), 13.8 (CH$_3$).

2,2′-Bipyridine-5,5′-dicarboxylic Diazide (11): 50 mL of an 80% hydrazine hydrate solution was added to a slurry of 8.20 g (27.3 mmol) of **10** in 50 mL of ethanol. The mixture was heated for 3 h at an oil-bath temperature of 120°C to give a viscous mass which was filtered, washed with hot ethanol and dried in vacuo. The intermediate dihydrazide (6.5 g) thus obtained was suspended at 0°C in 150 mL of conc. HCl. A solution of 3.88 g (56 mmol) of NaNO$_2$ in 30 mL of water was added dropwise to this slurry with the temperature kept always below 10°C. After a few hours, a clear yellow solution was obtained. Upon dilution with 750 mL of water a colorless precipitate was produced which was filtered, washed several times with water, twice with 30 mL of hot ethanol and dried in vacuo to yield 6.72 g (84%) of a white powder. − M.p. > 300°C. − IR (Nujol): ṽ = 3076 cm^{-1} w, 2730 w, 2182 w, 2143 w, 1728 w,

1696 s, 1595 m, 1556 w, 1560 w, 1467 s, 1380 m, 1290 m, 1282, 1238 m, 1182 m, 1238 w, 1182 w, 1160 w, 1130 w, 1120 w, 1058 w, 1034 w, 1000 w, 895 w, 870 w, 860 w, 751 w, 722 w.

5,5′-Bis(ethoxycarbonylamino)-2,2′-bipyridine (12): 6.00 g (20.4 mmol) of the diazide **11** was suspended in a mixture of 150 mL of *p*-xylene and 150 mL of dried ethanol and refluxed for 18 h to give a clear yellow solution. Upon cooling yellowish crystals were obtained which after filtration were recrystallized from ethanol. The yield of the now colorless product was 6.5 g (97%). − M.p. > 300°C. − ^{1}H NMR ([D$_6$]DMSO): δ = 9.92 (s, 2 H, NH), 8.67 (d, 2 H, J = 2.2 Hz, H6, H6′), 8.20 (d, 2 H, J = 8.8 Hz, H3, H3′), 7.97 (dd, 2 H, J_1 = 8.8 Hz, J_2 = 2.4 Hz, H4, H4′), 4.14 (q, 4 H, J = 7.1 Hz, OCH_2CH$_3$), 1.24 (t, 6 H, J = 7.1 Hz, CH$_2$CH_3). − ^{13}C NMR ([D$_6$]DMSO): δ = 159.3 (EtOCONH), 155.0 (C2, C2′), 144.9 (C6, C6′), 141.5 (C4, C4′), 131.5 (C3, C3′), 125.6 (C5, C5′), 66.4 (OCH$_2$), 20.2 (CH$_3$).

5,5′-Diamino-2,2′-bipyridine (5): 5.00 g (15.2 mmol) of the diurethane **12** was refluxed for 24 h in a mixture of 200 mL of ethanol and 200 mL of 2 N NaOH. After cooling to room temperature, the solution was carefully neutralized and the alcohol distilled of at normal pressure. Upon cooling the hydrate of the diamine **5** crystallized as long needles which may be weakly pink colored due to traces of iron. Further purification was achieved by sublimation at 0.2 mbar and an oil-bath temperature of 190°C. Yield 1.97 g (70%). Analytical data are given after the following procedure.

Synthesis of 5 by Coupling of 5-Amino-2-chloropyridine (Scheme 2): In a 250-mL three-necked flask was placed 2.37 g (10 mmol) of nickel dichloride hexahydrate and 10.5 g (40 mmol) of triphenylphosphane. The flask was evacuated and refilled with argon for three times. 100 mL of dried dimethyl formamide was added under inert gas and the solution rapidly turned blue. After PPh$_3$ and NiCl$_2$ × 6 H$_2$O had completely dissolved in DMF, 0.7 g (11 mmol) of zinc powder was added to the solution under inert gas at 50°C and the solution slowly turned brown-red. After stirring this mixture for 1 h, 10 mL of a DMF solution with 1.28 g (10 mmol) of 5-amino-2-chloropyridine was added dropwise to the mixture. Stirring was continued for 4 h at 50°C at which time the starting material could not be detected anymore by thin-layer chromatography (eluent ethyl acetate). The reaction mixture was then concentrated in vacuo to half of its volume. After adding 250 mL of water, the mixture was carefully poured into 150 mL of conc. ammonia and stirred for 18 h. The solution turned blue because of the formation of hexaamminenickel(II) complexes. The PPh$_3$ precipate was removed by filtration and the filtrate was extracted three times with 50 mL of dichloromethane each. The combined organic phases were treated with 50 mL of half-concentrated HCl for three times each to separate the diaminobipyridine from PPh$_3$. During this procedure strongly colored aminohydrochlorides of **5** were formed. The combined acidic aqueous phases were carefully neutralized with a 10% Na$_2$CO$_3$ solution. The product **5** separated as a yellowish solid and was sublimed as described above to give a colorless powder (yield 1.11 g, 60%). − M.p. 205°C (ref.[12] 205−206°C). − ^{1}H NMR ([D$_6$]DMSO): δ = 7.92 (d, 2 H, J = 2.8 Hz, H6, H6′), 7.84 (d, 2 H, J = 8.6 Hz, H3, H3′), 6.95 (dd, 2 H, J_1 = 8.6 Hz, J_2 = 2.5 Hz, H4, H4′), 5.30 [s (br.), 4 H, NH$_2$]. − ^{13}C NMR (CDCl$_3$): δ = 144.7 (C2, C2′),143.6 (C5, C5′), 134.9 (C6, C6′), 120.5 (C3, C3′), 119.0 (C4, C4′); ([D$_6$]DMSO): δ = 147.1, 145.5, 136.6, 123.5, 122.2. − IR (KBr): ṽ = 3424 cm^{-1} w, 3338 m, 3310 m, 3207 m, 3062 w, 3057 w, 3005 w, 1632 w, 1600 m, 1568 m, 1478 s, 1412 m, 1289 m, 1248 w, 1137 w, 1108 w, 1088 w, 1060 w, 1024 w, 920 w, 897 w, 846 m, 832 m, 737 w, 656 m, 552 m, 517 m, 509 w, 418 w.

Syntheses of Transition Metal Complexes

[Tris(5,5′-diamino-2,2′-bipyridine)manganese(II)] Chloride Hydrate (14): To a solution of 76.2 mg (0.38 mmol) of MnCl$_2$ × 4 H$_2$O in 20 mL of distilled water was given a solution of 192.5 mg (1.03 mmol) of **5** in 25 mL of ethanol. The pale red solution was allowed to stand several days at room temperature. The bright red cubic crystals were separated by filtration. Upon standing in air the crystals slowly lose water of crystallization and turn opaque (yield 222 mg, 82%). − A thermogravimetric analysis shows the complete loss of crystal water at 101−145°C. At 290°C the loss of one diaminobipyridine ligand takes place with possible formation of [MnCl$_2$(**5**)$_2$]. Above 360°C decomposition is observed. − IR (Nujol): ṽ = 3420 cm^{-1} w (br.), 3305 m (br.), 3200 w (br.), 1632 m, 1598 s, 1585 m, 1487 m, 1430 m, 1325 w (br.), 1319 m, 1300 m, 1272 w (br.), 1262 w (br.), 1162 w, 1055 w, 1030 m, 1019 w, 965 w (br.), 890 w, 862 w, 852 w, 827 m, 758 w, 740 w, 728 m, 656 w, 650 w. − Tetrahydrate C$_{30}$H$_{38}$Cl$_2$MnN$_{12}$O$_4$ (756.56): calcd. C 47.62, H 5.06, N 22.21; found C 47.56, H 4.05, N 22.31.

[Diazidobis(5,5′-diamino-2,2′-bipyridine)manganese(II)] (15): 15 mL of an ethanolic solution of **5** (100 mg, 0.54 mmol) was added to 15 mL of an aqueous solution of MnCl$_2$ × 4 H$_2$O (110 mg, 0.54 mmol) and stirred for 15 min. To this solution was added 5 mL of an aqueous solution of NaN$_3$ (88 mg, 1.35 mmol). The resulting yellow solution was left standing for 36 h at room temperature. Then some undissolved solid was filtered and the filtrate was then placed at ambient temperature. One month later, a yellow precipate had formed on the bottom of the flask. Two months later, the yellow precipate had transformed into well-formed red-orange crystals which were collected by filtration and washed with water and ethanol to give 123 mg of product (69%, based on **5**). − IR (KBr): ṽ = 3430 cm^{-1} w, 3372 s, 3304 s, 3207 s, 2078 s ν(N$_3$), 2020 s ν(N$_3$), 1620 s, 1604 s, 1588 s, 1485 s, 1438 s, 1350 w, 1328 m, 1311 s, 1295 m, 1275 s, 1165 m, 1125 w, 1060 w, 1030 m, 1025 m, 960 w, 934 m, 892 m, 865 w, 849 m, 838 s, 728 m, 698 w, 653 m, 630 m, 620 w, 592 w, 545 s, 520 m. − C$_{20}$H$_{20}$N$_{14}$Mn (511.40): calcd. C 46.96, H 3.91, N 38.36; found C 46.76, H 3.92, N 38.33.

[Tris(5,5′-diamino-2,2′-bipyridine)iron(II)] Sulfate Hydrate (16): To a hot solution (90°C) of 532 mg (2.86 mmol) of **5** in 30 mL of distilled water was added dropwise a solution of 280 mg (1.01 mmol) of FeSO$_4$ × 7 H$_2$O in 10 mL of distilled water. A red color immediately developed. After complete addition, the solution was allowed to cool and the precipitated crystals were washed with a few mL of ice-cooled water, then with dried ethanol and finally with diethyl ether. The crystals were briefly dried in air. Single crystals could best be obtained by cooling a saturated solution from room temperature to 0°C (yield 720 mg, 92%). − A thermogravimetric analysis shows the complete loss of water of crystallization at 166°C and decomposition above 350°C. − ^{1}H NMR (D$_2$O): δ = 7.99 (d, J = 8.8, H3, H3′), 7.29 (dd, J_1 = 8.8 Hz, J_2 = 2.4 Hz, H4, H4′), 6.85 (d, J = 2.4 Hz, H6, H6′). − ^{13}C NMR (D$_2$O): δ = 149.6 (C2, C2′), 144.7 (C5, C5′), 139.3 (C6, C6′), 123.1 (C4, C4′), 121.4 (C3, C3′). − IR (Nujol): ṽ = 3420 cm^{-1} w, 3340 w, 3205 w, 1632 s, 1602 s, 1580 m, 1575 w, 1488 s, 1429 m, 1368 s, 1352 m, 1328 m, 1310 s, 1292 m, 1268 m, 1206 m, 1165 m, 1028 w, 1019 w, 904 w, 860 w, 838 w, 832 w, 728 w, 655 w. − Hexahydrate C$_{30}$H$_{42}$FeN$_{12}$O$_{10}$S (818.65): calcd. C 44.01, H 5.17, N 20.53; found C 44.16, H 4.20, N 20.50.

[Tris(5,5′-diamino-2,2′-bipyridine)nickel(II)] Chloride Hydrate (17): A solution of 158 mg (0.66 mmol) NiCl$_2$ × 6 H$_2$O in 30 mL of distilled water was combined with a solution of 383 mg (2.05 mmol) of **5** in 25 mL of ethanol. The mixture was heated to reflux and a pale red solution formed. After cooling to room

temperature, the precipitate was filtered, washed with little cold water, ethanol, and diethyl ether and air-dried (yield 150 mg, 85%). Single crystals could be obtained by slow cooling of a saturated solution from room temperature to 0°C. The product crystallizes in bright red cubes, which slowly loose water of crystallization in air. − A thermogravimetric analysis shows the complete loss of water of crystallization at 168°C and decomposition above 280°C. − IR (Nujol): $\tilde{\nu}$ = 3420 cm^{-1} w (br.), 3320 w (br.), 3200 m (br.), 1630 m, 1602 s, 1579 m, 1486 s, 1432 m, 1321 m, 1300 m, 1272 m, 1260 w, 1161 w, 1060 w, 1054 w, 1031 w, 1019 w, 960 w (br.), 888 w, 868 w, 852 w, 828 m, 722 w, 654 m, 596 w, 532 w, 428 w. − Hexahydrate $C_{30}H_{42}Cl_2N_{12}NiO_6$ (796.34): calcd. C 45.25, H 5.31, N 21.11; tetrahydrate $C_{30}H_{38}Cl_2N_{12}NiO_4$ (760.31): calcd. C 47.39, H 4.99, N 22.10; 2.5-hydrate $C_{30}H_{35}Cl_2N_{12}NiO_{2.5}$ (733.28): calcd. C 49.13, H 4.81, N 22.92; found C 47.64, H 4.08, N 22.39.

[Tris(5,5′-diamino-2,2′-bipyridine)nickel(II)] Thiocyanate (18): To an aqueous solution (100 mL) of NiCl$_2$ × 6 H$_2$O (0.64 g, 2.69 mmol or 0.32 g, 1.35 mmol) was added a DMF solution (10 mL) of **5** (0.50 g, 2.69 mmol). After stirring for 2 h, 50 mL of conc. ammonia was added and stirring was continued for 20 h. During this time the solution changed color from yellow to brown. 20 mL of the aforementioned solution (containing 80 mg/0.34 mmol or 40 mg/0.17 mmol of nickel and 62 mg/0.34 mmol of **5**) was used to overlayer 5 mL of an aqueous solution of 33 mg (0.34 mmol) of KSCN in a test tube. The solution was allowed to stand for 15 d at ambient temperature. The resulting orange-brown crystals were collected by filtration, washed with water and ethanol and dried under vacuum (yield 66−76 mg, 54−66% based on **5**). − $C_{32}H_{30}N_{14}NiS_2$ (733.50): calcd. C 52.41, H 4.09, N 26.75; found C 51.45, H 4.11, N 26.41. − IR (KBr): $\tilde{\nu}$ = 3438 cm^{-1} m, 3300 m, 3190 m, 2076 s ν(SCN), 2048 s ν(SCN), 1630 s, 1602 s, 1580 s, 1460 s, 1443 s, 1318 m, 1310 m, 1300 m, 1275 m, 1170 m, 1163 m, 1148 w, 1060 w, 1035 m, 1021 w, 858 w, 840 m, 825 m, 744 w, 725 m, 700 w, 660 s, 550 m. − $C_{32}H_{30}N_{14}NiS_2$ (733.50): calcd. C 52.41, H 4.09, N 26.75; found C 51.56, H 4.19, N 26.57.

$^1_\infty$[Diaqua(5,5′-diamino-2,2′-bipyridine)(μ-sulfato)copper(II)] Hydrate (19): A 25-ml flask was charged with mixture of CuSO$_4$ × 5 H$_2$O (135 mg, 0.54 mmol), **5** (100 mg, 0.54 mmol) and 10 mL of water, sealed and heated in an oil bath to 120°C for 48 h. After cooling, the dark-green crystals formed were collected by filtration and washed with water and ethanol. Concentration of the filtrate by slow evaporation of the solvent at room temperature for 8 d gave another crop of well-formed dark-green crystals. A total yield of 183 mg (89%) was obtained. − IR (KBr): $\tilde{\nu}$ = 3420 cm^{-1} m, 3340 m, 3220 m, 1650 m, 1606 m, 1590 m, 1495 s, 1446 w, 1332 w to m, 1324 w, 1280 w, 1210 w, 1140 m, 1115 m, 1040 w, 955 w, 925 w, 850 w, 839 w, 718 w, 660 w, 550 w. − $C_{10}H_{14}CuN_4O_6S$ (381.86): calcd. C 31.45, H 3.67, N 14.68; found C 31.32, H 3.84, N 14.70.

[Dichloro(5,5′-diamino-2,2′-bipyridine)copper(II)] (20): 10 mL of an aqueous solution of CuCl$_2$ × 2 H$_2$O (92 mg, 0.54 mmol) was carefully overlayered in a test tube with 10 mL of an ethanolic solution of **5** (100 mg, 0.54 mmol). The solution was allowed to stand for 7 d at room temperature. After this time, the well-formed rod-shaped dark-green crystals were collected by filtration and washed with cold water and ethanol to give 14 mg of product (82%). − IR (KBr): $\tilde{\nu}$ = 3448 cm^{-1} s, 3346 s, 3210 w, 1615 s, 1603 s, 1580 m, 1510 w, 1492 s, 1435 m, 1350 w to m, 1332 m, 1310 w, 1278 m, 1220 m, 1161 w, 1156 w, 1064 w, 1038 m, 1022 w, 968 w, 885 w, 836 s, 715 m, 665 w, 660 w, 550 m, 530 w. − $C_{10}H_{10}Cl_2CuN_4$ (322.66): calcd. C 37.44, H 3.12, N 17.47; found C 36.45, H 3.12, N 17.15. − The reaction of **5** in ethanol (or THF) with CuCl$_2$ × 2 H$_2$O in water in the molar ratio of 1:2 also gave **20**.

[(5,5′-Diamino-2,2′-bipyridine)dinitratozinc(II)] (21): A solution of 64 mg (0.22 mmol) of Zn(NO$_3$)$_2$ × H$_2$O in 5 mL of distilled water was overlayered in a test tube first with 2 mL of ethyl acetate and then with a solution of 35 mg (0.19 mmol) of **5** in 4 mL of ethanol. After standing for several days, colorless rhombohedra had formed at the boundary layer, which were carefully separated, washed with little THF and air-dried (yield 55 mg, 77%). − When **21** was heated with two equivalents of **5** in water crystals formed upon cooling which were shown by analysis to have a 3:1 ligand/metal ratio as in **22**.

[Tris(5,5′-diamino-2,2′-bipyridine)zinc(II)] Nitrate Hydrate (22): To a solution of 167.5 mg (0.56 mmol) Zn(NO$_3$)$_2$ × 6 H$_2$O in 20 mL of distilled water was added 332.8 mg (1.79 mmol) of **5** and the mixture heated to reflux for 30 min which led to a clear solution. After cooling to room temperature, the crystals formed were separated by filtration, washed with little ice-cooled water, ethanol and diethyl ether. After drying in air, the complex was obtained as a light yellow fine crystalline powder. Single crystals were obtained by slow cooling of a saturated solution from room temperature to 0°C (yield 320 mg, 69%). − A thermogravimetric analysis shows complete loss of the water of crystallization at 179°C and decomposition above 335°C. − ^{1}H NMR (D$_2$O):δ = 8.43 (d, J = 8.6, H3, H3′), 7.84 (dd, J_1 = 8.6 Hz, J_2 = 2.6 Hz, H4, H4′), 7.79 (d, J = 2.6 Hz, H6, H6′); ([D$_6$]DMSO): δ = 8.08 (d, J = 8.7, H3, H3′), 7.19 (dd, J_1 = 8.7 Hz, J_2 = 2.5 Hz, H4, H4′), 7.08 (d, J = 2.5 Hz, H6, H6′). − ^{13}C NMR (D$_2$O):δ = 145.5 (C2, C2′), 140.8 (C5, C5′), 134.4 (C6, C6′), 126.1 (C4, C4′), 122.2 (C3, C3′). − IR (Nujol): $\tilde{\nu}$ = 3430 cm^{-1} w (br.), 3325 w (br.), 3210 w (br.), 1630 m, 1602 s, 1582 m, 1488 m, 1378 m, 1342 m, 1320 m, 1316 m, 1272 m, 1160 w, 1152 w, 1142 w, 1080 w, 1060 w, 1031 w, 1019 w, 898 w, 892 w, 867 w, 850 w, 838 w, 828 m, 722 m, 658 w. − Dihydrate $C_{30}H_{34}N_{14}O_8Zn$ (784.07): calcd. C 45.94, H 4.37, N 25.00; found C 45.61, H 3.32, N 25.05.

[(5,5′-Diamino-2,2′-bipyridine)nitratosilver(I)] Hydrate (23): A solution of 122 mg (0.72 mmol) of AgNO$_3$ in 10 mL of distilled water was overlayered in a test tube first with 3 mL of dried ethyl acetate and then with a solution of 104 mg (0.56 mmol) of **5** in 15 mL of dried ethanol. After standing for several weeks at room temperature in the dark, yellowish fiber clusters had formed at the layer boundary. They were separated by filtration, washed with some cold water, ethanol and finally diethyl ether. Drying in air gave light yellow fibers (yield 1.66 mg, 76%). − M.p. > 195°C (dec.). − ^{1}H NMR ([D$_6$]DMSO): δ = 7.92 (d, J = 2.6 Hz, H6, H6′), 7.91 (d, J = 8.8 Hz, H3, H3′), 7.15 (dd, J_1 = 8.6 Hz, J_2 = 2.6 Hz, H4, H4′). − ^{13}C NMR ([D$_6$]DMSO): δ = 145.2 (C2, C2′), 140.4 (C5, C5′), 136.2 (C6, C6′), 121.9 (C4, C4′), 121.2 (C3, C3′). − IR (Nujol): $\tilde{\nu}$ = 3450 cm^{-1} w (br.), 3325 m (br.), 3210 w (br.), 1628 s, 1604 s, 1574 m, 1488 s, 1422 m, 1350 s, 1326 s, 1296 m, 1271 m, 1252 w, 1153 w, 1062 w, 1043 w, 1022 w, 1018 w, 879 w, 862 w, 843 w, 819 w, 722 m, 652 m, 646 m. − $C_{10}H_{14}AgN_5O_5$ (392.12): calcd. C 30.63, H 3.60, N 17.86; found C 30.22, H 3.18, N 17.63.

[Bis(5,5′-diamino-2,2′-bipyridine)silver(I)] Nitrate (24): A slurry of 225 mg (1.21 mmol) of **5** in 20 mL of distilled water was heated until complete dissolution. Then a hot solution of 110 mg (0.65 mmol) of AgNO$_3$ in 10 mL of water was added which immediately gave a colorless precipitate. This was shown by elemental analysis to have a 1:1 ligand/metal composition. Conc. aqueous ammonia was added dropwise until the precipitate had completely dissolved. The solution was kept at room temperature open to the air and after a few days thin platelets with a mother-of-pearl shine had formed. The crystals were collected by filtration, washed with diethyl ether and dried in vacuo (yield 171 mg, 52%). − M.p. >

230 °C. − ^{1}H NMR ([D$_6$]DMSO): δ = 7.91 (d, J = 8.6 Hz, H3, H3′), 7.90 (d, J = 2.3 Hz, H6, H6′), 7.12 (dd, J_1 = 8.6 Hz, J_2 = 2.6 Hz, H4, H4′), 5.68 [s (br.), NH$_2$]. − ^{13}C NMR ([D$_6$]DMSO): δ = 145.1 (C2, C2′), 140.7 (C5, C5′), 136.0 (C6, C6′), 121.8 (C4, C4′), 121.0 (C3, C3′). − IR (Nujol): ṽ = 3420 cm^{-1} w, 3340 w, 3205 w, 1632 s, 1602 s, 1582 m, 1575 w, 1488 s, 1429 m, 1368 s, 1352 m, 1328 m, 1310 s, 1292 m, 1268 m, 1206 m, 1165 m, 1028 w, 1019 w, 904 w, 860 w, 838 w, 832 w, 728 w, 655 w. − C$_{20}$H$_{20}$AgN$_9$O$_3$ (542.31): calcd. C 44.30, H 3.70, N 23.25; found C 44.73, H 3.95, N 23.46.

$^1_\infty$[Di(μ-chloro)(5,5′-diamino-2,2′-bipyridine)cadmium(II)] Hydrate (25): A solution of 175 mg (0.87 mmol) CdCl$_2$ × H$_2$O in 10 mL of distilled water was overlayered in a test tube first with 3 mL of ethyl acetate and then with a solution of 130 mg (0.70 mmol) of **5** in 15 mL of ethanol. After standing for several days, colorless rhombohedra had formed at the boundary layer, which were carefully separated, washed with little THF and air-dried (yield 160 mg, 56%). − M.p. > 225 °C. − ^{1}H NMR ([D$_6$]DMSO): δ = 7.98 [s (br.), H6, H6′], 7.92 (d, J = 8.7 Hz, H3, H3′), 7.14 (dd, J_1 = 8.7 Hz, J_2 = 2.7 Hz, H4, H4′), 5.85 [s (br.), NH$_2$]. − ^{13}C NMR ([D$_6$]DMSO): δ = 145.5 (C2, C2′), 138.0 (C5, C5′), 134.7 (C6, C6′), 122.8 (C4, C4′), 120.8 (C3, C3′). − IR (Nujol): ṽ = 3510 cm^{-1} w, 3338 m (br.), 3204 m (br.), 1638 m (br.), 1602 s, 1590 s, 1487 s, 1435 m, 1326 w, 1315 w, 1300 m, 1272 m, 1266 m, 1160 m, 1130 w (br.), 1064 w (br.), 1030 m, 918 m, 862 msh, 845 s, 827 m (br.), 727 m, 700 w, 655 w. − C$_{10}$H$_{14}$CdCl$_2$N$_4$O$_2$ (405.56): calcd. C 29.59, H 3.48, N 13.80; found C 30.55, H 3.22, N 13.23. − When **25** was heated with two equivalents of **5** in water crystals formed upon

cooling which were shown by analysis to have a 3:1 ligand/metal ratio as in **26**.

[Tris(5,5′-diamino-2,2′-bipyridine)cadmium(II)] Chloride Hydrate (26): In 20 mL of an aqueous solution of 117.5 mg (0.58 mmol) of CdCl$_2$ × H$_2$O was suspended 336.0 mg (1.80 mmol) of **5** and heated under reflux for 30 min. From the bright yellow solution fine crystals formed upon cooling, which were filtered, washed with little ethanol and diethyl ether and air-dried. Upon storage in air the crystals slowly lost incorporated solvent water (yield 350 mg, 76%). − M.p. > 225 °C. − ^{1}H NMR ([D$_6$]DMSO): δ = 7.90 (d, J = 8.6, H3, H3′), 7.88 (d, J = 2.6 Hz, H6, H6′), 7.09 (dd, J_1 = 8.6 Hz, J_2 = 2.6 Hz, H4, H4′). − ^{13}C NMR ([D$_6$]DMSO): δ = 144.9 (C2, C2′), 139.4 (C5, C5′), 134.6 (C6, C6′), 122.2 (C4, C4′), 120.4 (C3, C3′). − ^{113}Cd NMR (66.0 MHz, ([D$_6$]DMSO), standard is a 2.0 M cadmium perchlorate solution in D$_2$O): δ = 254 (s), half width 30 ppm. − IR (Nujol): ṽ = 3425 cm^{-1} w, 3310 w, 3205 w, 1628 s, 1604 m, 1586 w, 1495 s, 1440 s, 1330 m, 1322 w, 1280 w, 1269 w, 1172 w, 1168 w, 1130 w (br.), 1036 w, 1028 w, 970 w, 905 w, 888 w, 870 w, 833 m, 728 w, 668 w, 660 w. − Dihydrate C$_{30}$H$_{34}$CdCl$_2$N$_{12}$O$_2$ (778.00): calcd. C 46.29, H 4.40, N 21.59; found: C 45.59, H 3.85, N 21.48.

X-ray Structure Determinations: Data were collected with Mo-K_α radiation (λ = 0.71073 Å) and the use of a graphite monochromator. Structure solution was performed by direct methods using SHELXS-97.[65] Refinement: Full-matrix least-squares on F^2 [SHELXL-97 (version 97−2)];[65] all non-hydrogen positions found and refined with anisotropic temperature factors. Crystal data are

Table 5. Crystal data for compounds **15**−**20**, **22** and **25**

Compound	15	16	17	18	19	20	22	25
Empirical formula	C$_{20}$H$_{20}$N$_{14}$Mn	C$_{60}$H$_{96}$Fe$_2$N$_{24}$O$_{26}$S$_2$[f]	C$_{60}$H$_{70}$Cl$_4$N$_{24}$Ni$_2$O$_5$[f]	C$_{32}$H$_{30}$N$_{14}$NiS$_2$	C$_{10}$H$_{20}$CuN$_4$O$_9$S	C$_{10}$H$_{10}$Cl$_2$CuN$_4$	C$_{30}$H$_{34}$N$_{14}$O$_8$Zn	C$_{10}$H$_{14}$CdCl$_2$N$_4$O$_2$
M [g mol^{-1}]	511.405	2x872.68 [f]	2x733.28 [f]	733.500	435.899	322.665	784.07	405.56
Crystal size [mm]	0.45×0.35×0.25	0.50×0.30×0.05	0.80×0.50×0.40	0.25×0.15×0.09	1.08×0.15×0.09	0.46×0.08×0.08	0.76×0.39×0.25	0.30×0.20×0.20
Crystal description	prismatic	platelet	prismatic	prismatic	needle	needle	irregular	prismatic
Crystal color	red-brown	red	red	red	green	blue	yellow-brown	colorless
T [K]	200(3)	200(3)	200(3)	200(3)	200(3)	200(3)	200(3)	293(2)
Diffractometer	STOE-IPDS	STOE-IPDS	STOE-IPDS	STOE-IPDS	STOE-IPDS	STOE-IPDS	STOE-IPDS	Syntex P21
Scan type, 2 Θ range [°]	ω, 4.6−55.8	ω, 2.8−44.2	ω, 3.7−51.6	ω, 4.2−56.1	ω, 6.1−55.8	ω, 6.2−55.5	ω, 3.5−47.7°	ω, 8−40°
h; k; l range	−17, 17; −13, 14; −21, 20	−18, 18; −18, 18 −27, 27	−29, 29; −30, 24 −29, 27	−13, 13; −14, 14; −18, 18	−8, 9; −25, 25 −16, 16	−16, 16; −17, 17; −9, 9	−19, 12; −19, 19; −51, 48	0, 20; 0, 9; 0, 7
Crystal system	monoclinic	orthorhombic	monoclinic	triclinic	monoclinic	monoclinic	tetragonal	orthorhombic
Space group	I2/a	Pna2$_1$	C2/c	P1̄	P2$_1$/n	C2/c	I4$_1$/a	Pbcn
a [Å]	13.6751(13)	17.4099(11)	24.5144(18)	10.4923(11)	6.8693(6)	12.9032(11)	17.5457(12)	21.02(12)
b [Å]	10.8010(6)	17.2792(16)	24.8858(15)	11.2927(12)	11.4923(11)	19.4875(13)	17.5457(12)	9.40(4)
c [Å]	16.0833(14)	26.3756(18)	24.3872(19)	14.3883(14)	12.7217(10)	7.3981(6)	46.380(4)	7.32(4)
α [°]	90	90	90	79.264(12)	90	90	90	90
β [°]	114.136(10)	90	109.325(9)	74.867(12)	105.212(9)	112.987(9)	90	90
γ [°]	90	90	90	89.259(12)	90	90	90	90
V [Å^3]	2165.7(14)	7934(1)	14039(2)	1615.7(12)	1643.3(14)	1187.74(15)	14278.2(19)	1446(13)
Z	4	4	8	2	4	4	16	8
$D_{calcd.}$ [g cm^{-3}]	1.568(1)	1.4681(2)	1.3877(2)	1.508(1)	1.7619(15)	1.7933(2)	1.4590(2)	1.862
F(000) [electrons]	1052	3664	6096	760	900	644	6496	800
μ [$^{-1}$]	6.53	5.09	7.53	7.79	15.1	22.7	7.58	18.82
Absorption correction	numerical	numerical	numerical	numerical	numerical	numerical	numerical	empirical
Max/min transmission		0.830/0.980	0.687/0.786	0.874/0.935	0.390/0.861	0.739/0.863	0.619/0.753	0.759/0.643
Measured reflections	9648	39521	26958	15188	15509	3746	20364	666
Unique reflect. for refinemt. (R_{int})	2511 (0.0254)	9855(0.12)	12059(0.0485)	7146 (0.0258)	3890 (0.0831)	1045 (0.0275)	5421 (0.0568)	666 (0.0830)
Observed reflection [I > 2 σ(I)]	2234	7381	7354	5406	3431	939	4364	545
Parameters refined	199	482	897	562	306	98	492	88
Max/min Δρ[a] [e Å^{-3}]	0.386/−0.212	0.780/−0.489	1.225/−0.580	0.345/−0.316	1.037/−0.732	0.304/−0.219	0.496/−0.302	0.742/−0.576
R1/wR2[b] [I > 2 σ(I)]	0.0271/0.0701	0.087/0.226[g]	0.061/0.169	0.0304/0.0688	0.0311/0.0829	0.0205/0.0520	0.0386/0.0855	0.0489/0.1233
R1/wR2[b] (all reflections)	0.0313/0.0718	0.108/0.235	0.098/0.188	0.0467/0.0731	0.0355/0.0846	0.0235/0.0528	0.0516/0.0889	0.0528/0.1330
GOF on F^2[c]	1.046	1.090	0.931	0.918	1.006	1.058	0.945	0.972
Weighting scheme w: a/b[d]	0.0481/0.4789	0.109/26.376	0.1262/0.0000	0.0436/0.0000	0.0555/0.0000	0.0381/0.0000	0.0547/0.0000	0.1098/0.0000

[a] Largest difference peak and hole. − [b] Largest difference peak and hole. − [c] $R1 = (\Sigma F_o − F_c)/\Sigma F_o$; $wR2 = \{\Sigma[w(F_o^2 − F_c^2)^2] / \Sigma[w(F_o^2)^2]\}^{1/2}$. − [d] Goodness-of-fit, Gof = $\{\Sigma [w(F_o^2 − F_c^2)^2]/(n − p)\}^{1/2}$. − [e] $w = 1/[\sigma^2(F_o^2) + (a·P)^2 + b·P]$ where $P = [\max(F_o^2 \text{ or } 0) + 2·F_c^2]/3$. − [f] Two independent molecules in the unit cell. − [g] Structure refinement was hampered by the disorder in the anion-water layer.

listed in Table 5. The structure of compound **22** was refined as an axis twin (twin axis [010]). The volume fraction of the twin component from refinement was 0.5118(10), i.e. there is almost 1:1 twinning. Graphics were computed with ORTEP3 for Windows.[66] Crystallographic data (excluding structure factors) for the structures reported in this paper have been deposited with the Cambridge Crystallographic Data Center as supplementary publication no. CCDC-119339 (**15**), -119340 (**16**), -119341 (**17**), -119342 (**18**), 119343 (**19**), -119344 (**20**), -119345 (**22**), and -119346 (**25**). Copies of the data can be obtained free of charge on application to CCDC, 12 Union Road, Cambridge CB2 1EZ, UK [Fax: int. code + 44-1223/336-033; E-mail: deposit@ccdc.cam.ac.uk]. − Additional information (distances and angles) on hydrogen bonding which is not described in detail here can be found in the Supporting Information.

Acknowledgments

[1] A. E. Martell, R. D. Hancock, *Metal Complexes in Aqueous Solutions*, Plenum Press, New York, **1996**; A. v. Zelewsky, *Stereochemistry of Coordination Compounds*, Wiley, Chichester, **1996**; J. M. Lehn, *Supramolecular Chemistry*, VCH, Weinheim, **1995**.

[2] C. Janiak, L. Uehlin, H.-P. Wu, P. Klüfers, H. Piotrowski, T. G. Scharmann, unpublished work.

[3] H.-P. Wu, C. Janiak, G. Rheinwald, H. Lang, *J. Chem. Soc., Dalton Trans.* **1999**, 183−190.

[4] H.-P. Wu, C. Janiak, L. Uehlin, P. Klüfers, P. Mayer, *Chem. Commun.* **1998**, 2637−2638.

[5] For our recent work with the ambidente hydrotris(triazolyl)boate ligand see for example: C. Janiak, T. G. Scharmann, J. C. Green, R. P. G. Parkin, M. J. Kolm, E. Riedel, W. Mickler, J. Elguero, R. M. Claramunt, D. Sanz, *Chem. Eur. J.* **1996**, *2*, 992−1000. C. Janiak, T. G. Scharmann, H. Hemling, D. Lentz, J. Pickardt, *Chem. Ber.* **1995**, *128*, 235−244.

[6] C. B. Aakeröy, A. M. Beatty, *Chem. Commun.* **1998**, 1067−1068. C. B. Aakeröy, A. M. Beatty, D. S. Leinen, *J. Am. Chem. Soc.* **1998**, *120*, 7383−7384. C. B. Aakeröy, K. R. Sneddon, *Chem. Soc. Rev.* **1993**, *22*, 397−407.

[7] B.-H. Ye, X.-M. Chen, G.-Q. Xue, *J. Chem. Soc. Dalton Trans.* **1998**, 2827−2831.

[8] J. M. Lehn, M. Mascal, A. DeCian, J. Fischer, *Chem. Commun.* **1990**, 479. J. M. Lehn, M. Mascal, A. DeCian, J. Fischer, *J. Chem. Soc. Perkin Trans. 2* **1992**, 461−467. C. M. Drain, R. Fischer, E. G. Nolen, J. M. Lehn, *J. Chem. Soc., Chem. Commun.* **1993**, 243.

[9] P. G. Desmartin, A. F. Williams, G. Bernardinelli, *New. J. Chem.* **1995**, *19*, 1109−1112.

[10] B. Olenyuk, A. Fechtenkötter, P. J. Stang, *J. Chem. Soc., Dalton Trans.* **1998**, 1707−1728. L. R. MacGillivray, R. H. Groeneman, J. L. Atwood, *J. Am. Chem. Soc.* **1998**, *120*, 2676−2677. A. J. Blake, S. J. Hill, P. Hubberstey, W.-S. Li, *J. Chem. Soc., Dalton Trans.* **1998**, 909−915. M.-L. Tong, X.-M. Chen, X.-L. Yu, T. C. W. Mak, *J. Chem. Soc., Dalton Trans.* **1998**, 5−6. P. Stang, B. Olenyuk, *Acc. Chem. Res.* **1997**, *30*, 502−518. O. M. Yaghi, H. Li, T. L. Groy, *Inorg. Chem.* **1997**, *36*, 4292−4293. P. Lossier, M. J. Zaworotko, *Angew. Chem. Int. Ed.* **1996**, *35*, 2779−2782. O. M. Yaghi, H. Li, *J. Am. Chem. Soc.* **1996**, *118*, 295−296. C. A. Hunter, *Angew. Chem. Int. Ed. Engl.* **1995**, *34*, 1079−1081.

[11] C. Janiak, *Angew. Chem. Int. Ed. Engl.* **1997**, *36*, 1431−1434. O. M. Yaghi, H. Li, C. Davies, D. Richardson, T. L. Groy, *Acc. Chem. Res.* **1998**, *31*, 474−484.

[12] C. Whittle, *J. Heterocycl. Chem.* **1977**, *14*, 191−194.

[13] F. Ebmeyer, F. Vögtle, *Chem. Ber.* **1989**, *122*, 1725−1727. W. H. F. Sasse, C. P. Whittle, *J. Chem. Soc.* **1961**, 1347−1350.

[14] M. Badger, F. Sasse, *J. Chem. Soc.* **1956**, 616−620.

[15] F. Case, *J. Am. Chem. Soc.* **1946**, *68*, 2574−2576.

[16] M. Tiecco, L. Testaferri, M. Tingoli, D. Chianelli, M. Montaucci, *Synthesis* **1984**, 736−738. K. S. Chan, A. K.-S. Tse, *Synth. Commun.* **1993**, *23*, 1929−1934.

[17] Y. Fort, S. Becker, P. Caubère, *Tetrahedron* **1994**, *50*, 11893−11902.

[18] M. Lourak, R. Vanderesse, Y. Fort, P. Caubère, *J. Org. Chem.* **1989**, *54*, 4840−4844. M. Lourak, R. Vanderesse, Y. Fort, P. Caubère, *J. Org. Chem.* **1989**, *54*, 4844−4848.

[19] M. F. Semmelhack, P. Helquist, L. D. Jones, L. Keller, L. Menelson, R. Speltz-Ryono, J. Gorszynski-Smith, R. D. Staufer, *J. Am. Chem. Soc.* **1981**, *103*, 6460.

[20] C. O. Okafer, *J. Org. Chem.* **1973**, *38*, 4383−4386.

[21] C. Janiak, T. G. Scharmann, W. Günther, F. Girgsdies, H. Hemling, W. Hinrichs, D. Lentz, *Chem. Eur. J.* **1995**, *1*, 637−644.

[22] B. Jezowska-Trzebiatowska, H. Kozlowski, L. Latos-Grazynski, T. Kowalik, *Chem. Phys. Lett.* **1975**, *30*, 355−357.

[23] For a similar recrystallization reaction from aqueous ammonia, see C. Janiak, T. G. Scharmann, W. Günther, W. Hinrichs, D. Lentz, *Chem. Ber.* **1996**, *129*, 991−995. C. Janiak, T. G. Scharmann, P. Albrecht, F. Marlow, R. Macdonald, *J. Am. Chem. Soc.* **1996**, *118*, 6307−6308.

[24] A. Vertes, I. Deszi, M. Suba, *Acta Chim.* **1970**, *64*, 347−350.

[25] H. Sato, T. Tominaga, *Bull. Chem. Soc. Jpn.* **1976**, *49*, 697−700.

[26] C. Tänzer, R. Price, E. Breitmaier, G. Jung, W. Voelter, *Angew. Chem.* **1970**, *82*, 957−958.

[27] B. Jezowska-Trzebiatowska, G. Formicka-Kozlowska, H. Kozlowski, L. Latos-Grazynski, T. Kowalik, *Chem. Phys. Lett.* **1975**, *30*, 358−362.

[28] C. J. Jameson, J. Mason, in *Multinuclear NMR* (J. Mason, Ed.), Plenum Press, New York, **1989**, ch. 3, p. 72−74.

[29] M. Munakata, S. Kitagawa, F. Yagi, *Inorg. Chem.* **1986**, *25*, 964−970.

[30] P. F. Rodesiler, R. W. Turner, N. G. Charles, E. A. H. Griffith, A. L. Amma, *Inorg. Chem.* **1984**, *23*, 999−1004.

[31] C. Janiak in *Moderne Anorganische Chemie* (E. Riedel, Ed.), de Gruyter, Berlin, **1998**, ch. 2, p. 206.

[32] S. Vadera, N. Kumar, *J. Radioanal. Nucl. Chem.* **1990**, *146*, 29−35.

[33] L. Y. Johansson, R. Larsson, *Chem. Phys. Lett.* **1974**, *24*, 508−513.

[34] D. C. Craig, H. A. Goodwin, D. Onggo, *Aust. J. Chem.* **1988**, *41*, 1157−1169.

[35] Reviews: P. Gütlich, A. Hauser, H. Spiering, *Angew. Chem. Int. Ed. Engl.* **1994**, *33*, 2024−2054. O. Kahn, *Molecular Magnetism*, VCH, Weinheim, **1993**, ch. 4, p. 53ff. J. Zarembowitch, *New. J. Chem.* **1992**, *16*, 255−267. P. Gütlich, A. Hauser, *Coord. Chem. Rev.* **1990**, *97*, 1−22. H. Toftlund, *Coord. Chem. Rev.* **1989**, *94*, 67−108. E. König, *Progr. Inorg. Chem.* **1987**, *35*, 527−622. P. Gütlich, *Struct. Bonding (Berlin)* **1981**, *44*, 83−195. H. A. Goodwin, *Coord. Chem. Rev.* **1976**, *18*, 293−325.

[36] L. M. Eppstein, *J. Chem. Phys.* **1964**, *40*, 435−439.

[37] C. Janiak, T. G. Scharmann, T. Bräuniger, J. Holubova, M. Nadvornik, *Z. Anorg. Allg. Chem.* **1998**, *624*, 769−774.

[38] C. Janiak, *Chem. Ber.* **1994**, *127*, 1379−1385.

[39] S. Ahuja, R. Singh, C. Rai, *J. Molec. Struct.* **1978**, *49*, 201−205. G. C. Percy, D. Thornton, *J. Molec. Struct.* **1972**, *14*, 313. C. Postmus, J. Ferraro, W. Wozniak, *Inorg. Chem.* **1967**, *6*, 2030−2032. A. Schilt, R. Taylor, *J. Inorg. Nucl. Chem.* **1959**, *9*, 211−221.

[40] D. Thornton, G. Watkins, *J. Coord. Chem.* **1992**, *24*, 299−315.

[41] R. Inskeep, *J. Inorg. Nucl. Chem.* **1962**, *24*, 763−776.

[42] Gmelin, *Handbook of Inorganic Chemistry, Silver*, part B6, Springer Verlag, Berlin, **1975**, p. 91−95 and literature cited therein.

[43] E. Uhlig, M. Mädler, *Z. Anorg. Allg. Chem.* **1965**, *338*, 199−208.

[44] M. Muniz-Miranda, L. Angeloni, E. Castelluci, *Spectrochim. Acta* **1983**, *39A*, 97−106. M. Muniz-Miranda, E. Castelluci, *Spectrochim. Acta* **1983**, *39A*, 107−113.

[45] A. Wada, N. Sakabe, J. Tanaka, *Acta Crystallogr.* **1976**, *B32*, 1121−1127.

[46] X.-M. Chen, R.-Q. Wang, Z.-T. Xu, *Acta Crystallogr.* **1995**, *C51*, 820−822.

[47] U. Müller, *Struct. Bonding* **1973**, *14*, 141−172. Z. Dori, R. F. Ziolo, *Chem. Rev.* **1973**, *73*, 247−254. W. Beck, W. P.

Fehlhammer, P. Pöllmann, E. Schuierer, K. Feldl, *Chem. Ber.* **1967**, *100*, 2335−2361.

[48] M. V. Veidis, B. Dockum, F. F. Charron, Jr., W. M. Reiff, T. F. Brennan, *Inorg. Chim. Acta* **1981**, *53*, L197−L199.

[49] H. L. K. Wah, M. Postel, F. Tomi, L. Mordenti, D. Ballivet-Tkatchenko, F. Dahan, F. Urso, *New J. Chem.* **1991**, *15*, 629−633.

[50] S. Bernès, F. Sécheresse, Y. Jeannin, *Inorg. Chim. Acta* **1992**, *194*, 105−112.

[51] S. Decurtins, H. W. Schmalle, P. Schneuwly, H. R. Oswald, *Inorg. Chem.* **1993**, *32*, 1888−1892.

[52] H. W. Schmalle, R. Pellaux, S. Decurtins, *Z. Kristallogr.* **1996**, *211*, 533−538.

[53] S. Decurtins, H. W. Schmalle, P. Schneuwly, J. Ensling, P. Gütlich, *J. Am. Chem. Soc.* **1994**, *116*, 9521−9528.

[54] P. Román, C. Guzmán-Miralles, A. Luque, *J. Chem. Soc., Dalton Trans.* **1996**, 3985−3989.

[55] J. Cernak, E. Lenyelova, K. Ahmadi, A.-M. Hardy, *J. Coord. Chem.* **1996**, *37*, 55−58.

[56] J. Cernak, M. Kanuchova, J. Chomic, I. Potocnak, J. Kameicek, Z. Zak, *Acta Crystallogr.* **1994**, *C50*, 1563−1566.

[57] Recent examples of π-π interaction: N. Yoshida, H. Oshio, T. Ito, *Chem. Commun.* **1998**, 63−64. M. Lämsä, J. Huuskonen, K. Rissanen, J. Pursiainen, *Chem. Eur. J.* **1998**, *4*, 84−92; E. Ishow, A. Gourdon, J.-P. Launay, *Chem. Commun.* **1998**, 1909−1910. D. Ranganathan, V. Haridas, R. Gilardi, I. L. Karle, *J. Am. Chem. Soc.* **1998**, *120*, 10793−10800; cf. also refs.[3][4]

[58] G. V. Long, M. M. Harding, P. Turner, T. W. Hambley, *J. Chem. Soc., Dalton Trans.* **1995**, 3905−3910.

[59] R. Goddard, B. Hemalatha, M. V. Rajasekharan, *Acta Crystallogr. C* **1990**, *46*, 33−35.

[60] O. Gonzalez, A. M. Atria, E. Spodine, J. Manzur, M. T. Garland, *Acta Crystallogr. C* **1993**, *49*, 1589−1591.

[61] M. T. Garland, D. Grandjean, E. Spodine, A. M. Atria, J. Manzur, *Acta Crystallogr. C* **1988**, *44*, 1209−1212.

[62] S. Baggio, M. I. Pardo, R. Baggio, M. T. Garland, *Acta Crystallogr. C* **1997**, *53*, 1570−1572.

[63] U. Klement, D. Trumbach, H. Yersin, *Z. Kristallogr.* **1995**, *210*, 228. X.-M. Chen, R.-Q. Wang, X.-L. Yu, *Acta Crystallogr. C* **1995**, *51*, 1545−1547. E. Krausz, H. Riesen, A. D. Rae, *Aust. J. Chem.* **1995**, *48*, 929−932.

[64] G. V. Long, S. E. Boyd, M. M. Harding, I. E. Buys, T. W. Hambley, *J. Chem. Soc., Dalton Trans.* **1993**, 3195−3180.

[65] G. M. Sheldrick, *SHELXL-97, Program for Crystal Structure Refinement*, Göttingen **1997**; *SHELXS-97, Program for Crystal Structure Solution*, Göttingen, **1997**.

[66] M. N. Burnett, C. K. Johnson, *ORTEP-III, Oak Ridge Thermal Ellipsoid Plot Program for Crystal Structure Illustrations*, Oak Ridge National Laboratory Report ORNL-6895, **1996**. L. J. Farrugia, *ORTEP3 for Windows*, version 1.0.1β, University of Glasgow, Scotland, **1997**.